COLLISION STUDIES OF GASEOUS MOLECULAR LASERS

PRINCETON UNIVERSITY
PRINCETON, NEW JERSEY

DECEMBER 1976

Technical Report

Report No. Pr.-4

COLLISION STUDIES OF GASEOUS MOLECULAR LASERS

by

Herschel Rabitz

Department of Chemistry

Princeton University

December, 1976

Research Sponsored by the

Advanced Research Projects Agency

and the Office of Naval Research

under

Contract No. N0014-75-C-0478

Unclassified

SECURITY CLASSIFICATION OF THIS PAGE (When Data Entered)

REPORT DOCUMENTATION PAGE		READ INSTRUCTIONS BEFORE COMPLETING FORM
1. REPORT NUMBER Pr-4	2. GOVT ACCESSION NO.	3. RECIPIENT'S CATALOG NUMBER
4. TITLE (and Subtitle) COLLISIONAL STUDIES OF GASEOUS MOLECULAR LASERS		5. TYPE OF REPORT & PERIOD COVERED 6. PERFORMING ORG. REPORT NUMBER
7. AUTHOR(s) Herschel Rabitz		8. CONTRACT OR GRANT NUMBER(s) N0014-75-C-0478
9. PERFORMING ORGANIZATION NAME AND ADDRESS Princeton University Princeton, New Jersey 08540		10. PROGRAM ELEMENT, PROJECT, TASK AREA & WORK UNIT NUMBERS
11. CONTROLLING OFFICE NAME AND ADDRESS Director, Advanced Research Projects Agency 1400 Wilson Boulevard, Arlington Virginia 22209 Attention: Program Management		12. REPORT DATE December, 1976 13. NUMBER OF PAGES 4, and attached publications
14. MONITORING AGENCY NAME & ADDRESS (if different from Controlling Office) Office of Naval Research Arlington, Virginia 22217 Attention: Code 421		15. SECURITY CLASS. (of this report) Unclassified 15a. DECLASSIFICATION/DOWNGRADING SCHEDULE

16. DISTRIBUTION STATEMENT (of this Report)

Distribution unlimited

17. DISTRIBUTION STATEMENT (of the abstract entered in Block 20, if different from Report)

18. SUPPLEMENTARY NOTES

19. KEY WORDS (Continue on reverse side if necessary and identify by block number)

Vibration-Rotation Relaxation

Collision Theory

20. ABSTRACT (Continue on reverse side if necessary and identify by block number)

Collisional relaxation studies under way at Princeton are reviewed. Three areas of research are involved.

(1) Kinetic analysis of the CO laser system with updated rate information
(2) Model studies to determine the key molecular parameters controlling collisional behavior
(3) A stochastic theory for molecular collisions
(4) Vibration-Rotation Collisions in H_2-H_2

DD FORM 1 JAN 73 1473 EDITION OF 1 NOV 65 IS OBSOLETE

S/N 0102-LF-014-6601

SECURITY CLASSIFICATION OF THIS PAGE (When Data Entered)

REPORT SUMMARY

Research is under way in several areas of collision phenomena relevant to molecular laser operation. Due to the diverse nature of these problems, a multi-faceted approach has been taken. This has led to the study of both specific and model molecular systems in order to understand the physical phenomena involved. We believe the ensuing results have important implications for the development of high-power, efficient molecular lasers. In addition, a better overall fundamental understanding of molecular collisions has been gained and this should have application to a number of other relaxation phenomena. The remainder of this report consists of three manuscripts detailing specific aspects of this research performed in the past year. A brief summary of these results is given below.

1. Kinetic Analysis of the CO Laser System with Updated Rate Information

In collaboration with Professor E. Fisher, Wayne State University, we have undertaken a thorough examination of the kinetics in the low-temperature CO-He discharge system. This system has been suggested as an efficient source of high-power infrared laser radiation. Our present research focuses on an analysis of the observed CO population distribution and its implications for collisional rate behavior. This study has made important use of our recently calculated CO rate constants which show significant scaling differences with the older semiempirical models. The attached report presents a simple and useful correlation of the newly available rate information. This correlation is presently being used in CO laser analysis and the preliminary conclusion is that the new rate scalings make a substantial improvement in

explaining the observed CO population. It is our ultimate goal to turn this information around and suggest design improvements for operating laser systems. Further research in this area will be pursued in the coming year.

2. Model Studies to Determine the Key Molecular Parameters Controlling Collision Behavior

A variety of model calculations have been performed to bring out key physical effects entering into molecular collisions. A prime concern is the determination of temperature and quantum number scaling behavior. This information is very important in laser analysis and other general relaxation phenomena. A new and more accurate computer code has been written to replace our earlier version [J. Chem. Phys. 64, 5291 (1976)]. Calculations are presently under way and will be report d at a later date.

3. Stochastic Theory for Molecular Collisions

In the past few years the development of powerful effective Hamiltonian methods has greatly simplified molecular collision calculations. Indeed many previously impossible problems are now manageable with these methods and we have applied them in the research of this contract. However, the present available theory has limitations, particularly concerning the size of problem that can be handled. This restriction is very important in many practical applications such as lasers. Therefore, we have undertaken a new approach based on stochastic theory to handle large (many-quantum level) collision problems. The attached manuscript presents the stochastic theory formulation for vibration-rotation collision state changes. The paper discusses the physical content of the new simplified theory and suggests numerical methods

for its implementation. Applications are under way and will be pursued further in the coming year.

4. Vibration-Rotation Collisions in H_2-H_2

The H_2-H_2 system provides a valuable prototype example for many collisional effects of importance in lasing systems. Detailed three-dimensional quantum mechanical calculations were performed on this system with emphasis on the exchange of rotational and vibrational quanta between the molecules. Collisional flux maps were studied to determine the referred pathways for vibration-rotation transitions. This study has led to valuable insight into the collision of identical molecules. The details of this work are included in the attached manuscript. It would be valuable to extend this study to the collision of non-identical molecules such as D_2-H_2, since such situations commonly arise in many applications such as lasers. Further consideration of this work will be treated in the coming year.

CORRELATIONS OF VIBRATION-TRANSLATION RATES FOR CO-He

by

S. H. Lam

Department of Aerospace and Mechanical Sciences

and

H. Rabitz

Department of Chemistry

Princeton University, Princeton, New Jersey

September 1976

ABSTRACT

A new correlation of the recent theoretical CO-He vibration-translation rates by Verter and Rabitz is presented. Using a functional form suggested by the SSH theory, a simple analytical correlation function is obtained for $3000°K \geq T \geq 100°K$ and quantum state change $\Delta i = 1,2,3$. In addition, a semi-empirical formula for $\Delta i = 1$ rates is obtained by fine tuning the correlating formula to agree with the available experimental 1 to 0 rates. In this fashion optimal use was made of the best available theoretical and experimental information. The result is compared with rates estimated by other procedures.

CORRELATION OF VIBRATION-TRANSLATION RATES FOR CO-He

by

S. H. Lam* and H. Rabitz**

I. INTRODUCTION

In the study of vibrational kinetics of CO laser systems, quantitative information on various vibrational rates are required. A reexamination of the CO V-T (vibration-translation) information at this time is appropriate because of its importance in laser studies and because new theoretical[1] and experimental results[2] have recently become available. In the present paper, we shall be solely concerned with V-T rates for CO-He collisions, particularly at low temperatures T and high vibrational quantum numbers i. Our objective here is to construct and present a simple semi-empirical formula for the estimation of these rates based on the best theoretical and experimental information at our disposal at this time. The proposed semi-empirical formula, in addition to being of practical usefulness, exhibits certain general features where are interesting theoretically and are expected to be present in other similar systems.

---

*Department of Aerospace and Mechanical Sciences, Princeton University, Princeton, N. J.

**Alfred P. Sloan Fellow, Camille and Henry Dryfus teacher scholar, Department of Chemistry, Princeton University, Princeton, N. J.

We shall denote $k^{VT}(i,T;\Delta i)$ to be the de-excitation rate of a CO molecule from i to i-Δi at temperature T. The corresponding Δi to 0 rates shall be denoted simply by $k^{VT}_{\Delta i,0}(T)$.

Experimental data for $k^{VT}_{1,0}(T;exp)$ is relatively abundant, covering a wide range of temperature.[2,3,4] Experimental data for i≠1 rates is generally scarce, and for CO-He the totality of data appears to consist of only 5 points obtained by G. Hancock and Smith[5] (for i=9,10,11,12,13). Thus, estimation of rates for i≥1 and Δi≥1 in practical applications must rely primarily on guidance from theoretical considerations.

II. THE SSH THEORY AND THE BR ESTIMATION PROCEDURE

The vibrational levels E_i of CO may be written approximately as follows

$$E_i = ik\theta_v\left[1-x_e(i-1)\right], \quad i = 0,1,2,\ldots$$

where θ_v = 3123°K is the characteristic vibrational temperature and $x_e = 5.98 \times 10^{-3}$ is the anharmonicity which, inspite of its smallness, exerts a strong influence on the V-T rates.

The basic theory on vibrational rates was developed in a sequence of two papers by Schwartz, et al.[6,7] commonly referred to as the SSH theory. The SSH result for Δi=1 V-T rates can be written in the following form:

$$k^{VT}(i,T;1) = \omega_1(T)\ell_1(i)A_1^{VT}(y,T) \qquad (2.1)$$

where $\omega_1(T)$ carries the dimension of k^{VT} and contains mainly the total collision rate. The function $\ell_1(i)$ is proportional to the square of the appropriate oscillator matrix element which, for anharmonic oscillators,

can be approximated by

$$\ell_1(i) = \frac{i}{1-x_{ei}} \tag{2.2}$$

and $A_1^{VT}(y,T)$ is the so-called adiabaticity factor. The parameter y is defined by

$$y = y(i,T) = (1-2x_{ei}) \sqrt{\frac{\theta}{8T}} \tag{2.3}$$

where θ depends on molecular parameters and the assumed interaction potential. For a repulsive exponential interaction potential with characteristic length ℓ, θ is given by

$$\theta = 16\pi^4 \mu \ell^2 k \theta_v^2 / h^2 \tag{2.4}$$

where μ is the reduced mass of the collision. Using the analytical result of Jackson and Mott[8] and approximately accounting for 3-dimensionality effects[7], the SSH theory yields the following expression for $A_1^{VT}(y,T)$:

$$A_1^{VT}(y,T) = e^{\frac{\Delta E_i}{2kT}} f(y,z) \tag{2.5}$$

where $\Delta E_i = (1-2x_{ei})k\theta_v$ is the energy defect and f(y,z) is the thermal averaging integral

$$f(y,z) = \int_{2y/z}^{\infty} e^{-\xi} I(\xi;y,z) d\xi \tag{2.6}$$

with

$$I(\xi;y,z) = \frac{4\left(\sinh z \sqrt{\xi + \frac{2y}{z}}\right)\left(\sinh z \sqrt{\xi - \frac{2y}{z}}\right)}{\left[\cosh z \sqrt{\xi + \frac{2y}{z}} - \cosh z \sqrt{\xi - \frac{2y}{z}}\right]^2} \tag{2.7}$$

and

$$z = z(T) = 4\pi^2 \mu \left(\frac{2kT}{\mu}\right)^{\frac{1}{2}} \ell/h. \tag{2.8}$$

In the limit as $z \to \infty$, $I(\xi,y,\infty)$ reduces to $\sinh^{-2}(y/\sqrt{\xi})$, and $f(y,\infty)$ becomes

$$f(y,\infty) = \int_0^\infty e^{-\xi}\left(\sinh^{-2}(y/\sqrt{\xi})\right)d\xi \tag{2.9}$$

The function $f(y,\infty)$ has been numerically evaluated by Keck and Carrier[9] who suggest the following curve-fitting formula

$$f(y,\infty) \cong F_{KC}(y), \quad 0 \le y < 20, \tag{2.10}$$

$$F_{KC}(y) = 1/2\left(3-e^{-2y/3}\right)e^{-2y/3} \tag{2.11}$$

Eq. (2.11) is commonly preferred over the steepest-descent result, $8(\pi\, y^7/3)^{1/3}e^{-3y^2/3}$, $(y>>1)$, because of its uniform validity in the indicated range.

An estimation procedure for V-T rates, apparently first used by Bray[10] for high temperature and later more extensively developed by Rich[11] and co-workers[12], for low temperature proceeds as follows. First, the function $F_{KC}(y)$ is adopted to represent $f(y,z)$. The value of θ (or ℓ) is either estimated or taken from tabulated data (e.g., Herzfeld and Litovitz[13]). The factor $\omega_1(T)$ is then determined empirically by fitting the resulting formula for $i=1$ to the relatively abundant experimental data on $k^{VT}_{1,0}(T;\text{exp})$. If additional $i \neq 1$ data are available, they are used as a consistency check. We shall call this method the BR estimation procedure.

Note that the BR estimation procedure relies primarily on $F_{KC}(y)$ for the major i and T scaling, and the final formula contains a single molecular parameter, θ. A large number of kinetic calculations have adopted this procedure because of its simplicity and because of the absence of any better estimates.

Recently, Verter and Rabitz[1] (VR) performed extensive numerical calculations of V-T rates for CO-He collisions over the range 3000°K $\geq T \geq$ 100°K and $1 \leq i \leq 44$, including $i = 1, 2, 3$. These ab initio calculations provide for the first time detailed theoretical information hitherto unavailable. Although further refinements in the calculations are possible (at considerable additional expense), these results are believed to be the best theoretical CO-He rates presently available.

Verter and Rabitz correlated their computed results in the following form:

$$k^{VT}(i,T;\Delta i) = i \exp \sum_{n=0}^{4} B_n(T,\Delta i) i^{n-1} \qquad (2.12)$$

To cover the range 3000° $\geq T \geq$ 100°K in 100°K increments for $\Delta i = 1, 2, 3$, a total of 450 coefficients (B_n's) were needed. In this form the VR results are somewhat cumbersome to use and difficult to generalize or interpolate. Comparison of VR and experimental $k^{VT}_{1,0}(T)$ rates shows agreement with a factor of about 5 at high temperatures and a factor of about 2 at low temperatures. Comparison between the VP rates and the commonly used BR rates shows substantial differences, particularly at high values of i and low temperatures. These differences can have significant effects on kinetic modelling in CO laser studies as shall be pointed out later.

III. NEW CORRELATION OF THE VR DATA

Motivated by Eq. (2.1), we propose the following expresion as an alternative to Eq. (2.12):

$$k^{VT}(i,T;\Delta i) = \omega_{\Delta i}(i,T)\ell_{\Delta i}(i)e^{\frac{\Delta i \Delta E_i}{2kT}} F_{\Delta i}(y,T) \qquad (3.1)$$

where $\ell_1(i)$ remains as given by Eq. (2.2) and ℓ_2, ℓ_3 are chosen to be,[6]

$$\ell_2(i) = \ell_1(i)\ell_1(i-1), \quad \ell_3(i) = \ell_1(i)\ell_1(i-1)\ell_1(i-2) \tag{3.2}$$

The function $F_{\Delta i}(y,T)$ is to be chosen under the guiding principle that $\omega_{\Delta i}(i,T)$ should have the minimum i dependence. We shall retain y as defined by Eq. (2.3) as the primary correlation variable. The parameter θ affects y only by a constant factor and need not be specified in the correlation procedure. In fact, we shall presently determine an effective θ as a by-product of our correlations.

Inspection of the VR data appropriately reduced and plotted immediately indicates that the $\Delta i = 1$ high temperature data can indeed be roughly correlated by $F_{KC}(y)$ provided we choose $\theta = 2.64 \times 10^6$. Fixing θ at this value (which corresponds to $\ell = 0.3$ Å), the following form for $F_{\Delta i}(y,T)$ is proposed.

$$F_{\Delta i}(y,T) = \frac{3}{2}\left\{\frac{e^{-\alpha y}}{1+e^{a_1\alpha(y-a_2)}} + \frac{e^{-\alpha y_* - \alpha b_1(y-y_*)}}{1+b_2 e^{b_3[y-y(1,T)]}}\right\} \tag{3.3}$$

where α, a_1, a_2, b_1, b_2, b_3, and y_* are curve-fitting parameters. The first term is suggested by $F_{KC}(y)$ and dominates in the $y < y_*$ region. The second term dominates in the $y > y_*$ region. The parameters are found to be

$$\begin{aligned} &\alpha(\Delta i=1) = 2/3, \quad \alpha(\Delta i=2) = 1.03, \quad \alpha(\Delta i=3) = 1.3 \\ &a_1 = (2/3)^{\frac{1}{2}}, \quad a_2 = 5.5 \\ &y_* = 21.5 \qquad b_1 = 0.525\left(1 + \frac{24\alpha}{T}\right) \\ &b_2 = \left(\frac{280}{T}\right)^2, \quad b_3 = \frac{150}{T}. \end{aligned} \tag{3.4}$$

Note that $\theta = 2.64 \times 10^6$ °K is obtained as a consequence of setting $\alpha(\Delta i=1) = 2/3$.

Using this specific choice of $F_{\Delta i}(y,T)$, the values of $\omega_{\Delta i}(i,T)$ are then computed and typical distributions are shown in Fig. 1. It is seen that the resulting $\omega_{\Delta i}(i,T)$'s generally do exhibit a weak i dependence. As shall be seen more clearly later in Fig. 3, the exceptional cases are $\omega_1(1,100°K)$, $\omega_2(i<10,\ T<400°K)$, and $\omega_3(i<10,\ T<1000°K)$ where the correlation becomes locally poor. It is believed that for $\Delta i = 3$ the form for $\ell_3(i)$ assumed in Eq. (3.2) is mainly responsible for these large local aberations. For the other cases, the local aberations may be reduced by fine tuning the parameters b_2 and b_3. Since the original VR data for these cases is likely to have the largest numerical errors (noise), such refinements were not considered meaningful or worthwhile at this time.

Fig. 2 shows $\bar{\omega}_{\Delta i}(T)$ vs T where $\bar{\omega}_{\Delta i}(T)$ is the averaged value of $\omega_{\Delta i}$ $(10 \leq i \leq 40, T)$. Fig. 3 shows $F_{\Delta i}(y,T)$ as given by Eq. (3.3) vs y as solid lines. The original VR data represented by $F_{\Delta i}(y,T)\omega_{\Delta i}(i,T)/\bar{\omega}_{\Delta i}(T)$ may also be displayed on this diagram. However, because of the scale of the diagram, only the data with $\omega_{\Delta i}(i,T)/\bar{\omega}_{\Delta i}(T)$ substantially different from unity will deviate from the solid lines and is shown by the dotted lines.

IV. INCORPORATION OF EXPERIMENTAL DATA FOR $\Delta i = 1$

The weak "scatter" of $\omega_1(i,T)$ about $\bar{\omega}_1(T)$ is comparable to the scatter of the original VR calculations. Thus we may justifiably replace $\omega_1(i,T)$ in Eq. (3.1) by $\bar{\omega}_1(T)$ and consider the resulting formula as an alternative to Eq. (2.12) when $\Delta i = 1$.

Borrowing the idea from the BR estimation procedure, we propose the following semi-empirical formula for $k^{VT}(i,T,1)$:

$$k^{VT}(i,T;1;emp) = \omega_1(T;exp)\ell_1(i)e^{\frac{\Delta E_i}{2kT}} F_1(y,T) \qquad (4.1)$$

The function $\omega_1(T;exp)$ is to be determined by fitting the available experimental data on $k^{VT}_{1,0}(T;exp)$ while $F_1(y,T)$ determined from the VR theory is retained. Fig. 4 is a conventional plot of log $k^{VT}_{1,0}$ vs $T^{-1/3}$, showing the high temperature experimental data of Millikan and White[3] and the moderate and low temperature data of Miller and Millikan[4] and the recent data of Drozdoski, Young, Bates, and Hancock.[2] Also shown are the original VR rates.

Using the experimental data shown in Fig. 4, the values of $\omega_1(T;exp)$ are computed and are shown in Fig. 5. Also shown are $\omega_1(1,T)$ and $\bar{\omega}_1(T)$ for comparison purposes. The $\omega_1(T;exp)$ data can adequately be fitted by

$$\omega_1(T,exp) \tilde{=} A\left(\frac{T}{800}\right)^2, \quad 100°K \leq T \leq 800°K \qquad (4.2a)$$

$$\tilde{=} A\left(\frac{800}{T}\right)^{1/3} \quad 800°K \leq T \leq 3000°K \qquad (4.2b)$$

where

$$A = 6 \times 10^{13} \text{ cm}^3/\text{sec-molecule}$$

$$= 1 \times 10^{-10} \text{cm}^3/\text{sec-mole}.$$

In the indicated temperature range, Eqs. (4.1) and (4.2) is the proposed semi-empirical CO-He V-T rate formula which contains the most up-to-date theoretical and experimental information available at this time.

Fig. 6 shows $k^{VT}(i,T;1;emp)$ and the corresponding BR rates (using $\theta=2.64 \times 10^6$K) for T = 100°K, 200°K, and 300°K. Also shown are the

five data points of G. Hancock and Smith[5] which are believed to have been obtained at room temperature. Unfortunately, these data points do not discriminate between the two rate estimates which diverge from each other substantially only at higher vibrational levels. Thus, definitive confirmation of the VR rates must await additional discriminating experimental data to become available.

V. DISCUSSION

We have obtained a new correlation of the theoretical VR rates for CO-He in a form suggested by the SSH theory. For the $\Delta i = 1$ case, we have further proposed to replace $\omega_1(i,T)$ by $\omega_1(T;emp)$ given by Eq. (4.2) so that the resulting semi-empirical formula, Eq. (4.1), reproduces the experimental data on $k^{VT}_{1,0}(T;exp)$.

Using harmonic oscillator wave functions, the SSH theory showed that the square of the matrix elements can be written as $\ell_1(i) = i$, $\ell_2(i) = i(i-1)$. Our choice of $\ell_{\Delta i}(i)$ here rests entirely on analogy, accounting for the effects of anharmonicity only through the denominator of Eq. (2.2). We believe that the poor correlation of the low i data for the $\Delta i = 3$ case is primarily a reflection of the inadequacy of our choice of $\ell_3(i)$.

In addition to the constant θ used in the definition of y, the function $F_{\Delta i}(y,T)$ contains seven curve-fitting parameters: α, a_1, a_2, y^*, b_1, b_2, b_3. The values of α and θ are not independent. By setting $\alpha(1) = 2/3$ and requiring $F_1(y,T)$ to agree with $F_{KC}(y)$ for $10 < y < 20$, we deduce $\theta = 2.64 \times 10^6$ °K, yielding from Eq. (2.4) an effective interaction length $\ell = 0.3$ Å which is found to be in good agreement with the

actual interaction potential (in the strongly repulsive wall region) used in the original VR theory. The other curve-fitting parameters are probably also related to the interaction potential used, but such relationships have not been identified.

Using $\theta = 2.64 \times 10^6$ °K for CO-He collisions, the values of y for the temperatures range considered covers the range $57 > y > 5$. Since $F_{KC}(y)$, as given by Keck and Carrier,[9] is a valid approximation to $f(y,z)$ only for $y < 20$, we have numerically computed $f(y,z)$ as given by Eqs. (2.6) and (2.7) Our results show that for $y < 20$, $f(y,z)$ is indeed accurately represented by $F_{KC}(y)$. For $y > 20$, $f(y,z)$ exhibits a weak T dependence similar to $F_1(y,T)$, but diverges rapidly from it with increasing y.

An interesting feature of the VR rates is the distinctly more rapid variation of $F_{\Delta i}(y,T)$ with y for the first few levels when $y > y_* = 21.5$. Ignoring the $\Delta i = 3$ case which was discussed earlier, this distinctive "boundary layer" structure for low values of i can be clearly seen in Fig. 3. This behavior is accounted for by the denominator of the second term in Eq. (3.3), and the parameters $b_2(T)$ and $b_3(T)$ were chosen to fit the $\Delta i = 1$, 100°K and 200°K data. Since no such behavior is anticipated by the SSH theory, we have carefully examined the possibility of systematic numerical errors in the original VR calculations and concluded that it is unlikely. However, because of the complexities of the numerical procedures used, this possibility, although remote, cannot be entirely ruled out.

Except for this boundary layer structure (for $y > y_*$), the VR data is qualitatively consistent with the interpretation that the effective

value of ℓ is a variable and decreasing function of the "energy defect" of the collision.

While the reasonable agreement between the original VR rates with $k_{1,0}^{VT}(T;exp)$ as shown in Fig. 4 is encouraging, it must be emphasized that no definitive verifications at high values of i are yet available. The consistency check with the data of G. Hancock and Smith[5] is inconclusive. Nevertheless, it is clear that the semi-empirical rates (Eqs. (4.1) and (4.2) proposed here rest on firmer grounds than the BR rates. Recently, Lordi and Rich[14] measured CO population distributions in a CO-A laser system at 300°K up to i = 35 and compared their data with kinetic calculations. It was reported that calculations using BR rates yielded generally poor results, but calculations using the ad hoc assumption of replacing $F_{KC}(y)$ by a constant yielded much more reasonable results. Since the VR rates exhibit a generally weaker i dependence than the BR rates (see Fig. 6), their observation lends some support to the VR rates. The full implications of these new rates on CO laser calculations will be discussed in a later publication.

ACKNOWLEDGEMENT

This research was partially supported by ONR and ARPA (N0014-75-C-0478), AFOSR (F44620-73-0059), and the donors of the Petroleum Research Fund administered by the American Chemical Society.

REFERENCES

[1]M. Verter and H. Rabitz, J. Chem. Phys. 64 2939 (1976). The rates were calculated using three-dimensional quantum mechanical close-coupling methods. An electron-gas intermolecular potential was used and rotational states were ignored in the calculation.

[2]W. S. Drozdoski, R. M. Young, R. D. Bates, Jr., and J. K. Hancock, Temperature-Dependent Relaxation of CO(V=1) by HD, D_2, and He, and of D_2(V=1) by D_2. Presented at the 1976 APS Annual Meeting, New York (Feb. 1976).

[3]R. C. Millikan and D. R. White, J. Chem. Phys. 39, 98, (1963). Note that the logarithmic slope with respect to $T^{-1/3}$ as tabulated for CO-He was 99. In our study we use 78.3 which appears to fit the data better.

[4]D. J. Miller and R. C. Millikan, J. Chem. Phys. 53, 3384, (1970).

[5]G. Hancock and I. W. M. Smith, Applied Optics, 10, 1827, (1971).

[6]R. N. Schwartz, Z. I. Slawsky, and K. F. Herzfeld, J. Chem. Phys. 20, 1591, (1952).

[7]R. N. Schwartz and K. F. Herzfeld, J. Chem. Phys. 22, 767, (1954).

[8]J. M. Jackson and N. F. Mott, Proc. Roy. Soc., (London), A137, 703, (1932).

[9]J. Keck and G. Carrier, J. Chem. Phys. 43, 2284, (1965).

[10]K. N. C. Bray, J. Phys., B, Atom. Molec. Phys. 1, 705, (1968); also 3, 1515, (1970).

[11]J. W. Rich, J. Appl. Phys. 42, 2719, (1971).

[12]J. W. Rich, J. A. Lordi, R. A. Gibson, and S. W. Kang, Calspan Corp. Rept. WG-5134-A-3 (1974).

[13]K. F. Herzfeld and T. A. Litovitz, *Absorption and Dispersion of Ultrasonic Waves*, Academic Press, N. Y. (1959).

[14]J. A. Lordi and J. W. Rich, Claspan Corp. Report AFAL-TR-75-184, (1975).

FIGURE CAPTIONS

Fig. 1 Typical distributions of $\omega_{\Delta i}(i,T)$ as a function of i. A flat distribution indicates good correlation.

Fig. 2 $\bar{\omega}_{\Delta i}(T)$ as a function of T where $\bar{\omega}_{\Delta i}(T)$ is $\omega_{\Delta i}(i,T)$ averaged over the levels.

Fig. 3 The solid lines are $F_{\Delta i}(y,T)$. The dotted lines are $F_{\Delta i}(y,T)\omega_{\Delta i}(i,T)/\bar{\omega}_{\Delta i}(T)$ which represent the original VR data. Because of the scale of the diagram, only the data with $\omega_{\Delta i}(i,T)/\bar{\omega}_{\Delta i}(T)$ substantially different from unity is shown.

Fig. 4 Comparison of theoretical and experimental rates.

Fig. 5 $\omega_1(T,\text{exp})$, $\bar{\omega}_1(T)$ and $\omega_1(1,T)$ as a function of T. The solid dots are the recent data of Drozdoski, Young, Bates, and Hancock. The open circles are $\bar{\omega}_1(T)$. The crosses are $\omega_1(1,T)$. The solid curve is the data of Millikan and White. Straight line segments are given by Eqs. (4.2).

Fig. 6 Comparison of present semi-empirical rates with BR rates at low temperature. Note that the BR rates show a much stronger i dependence.

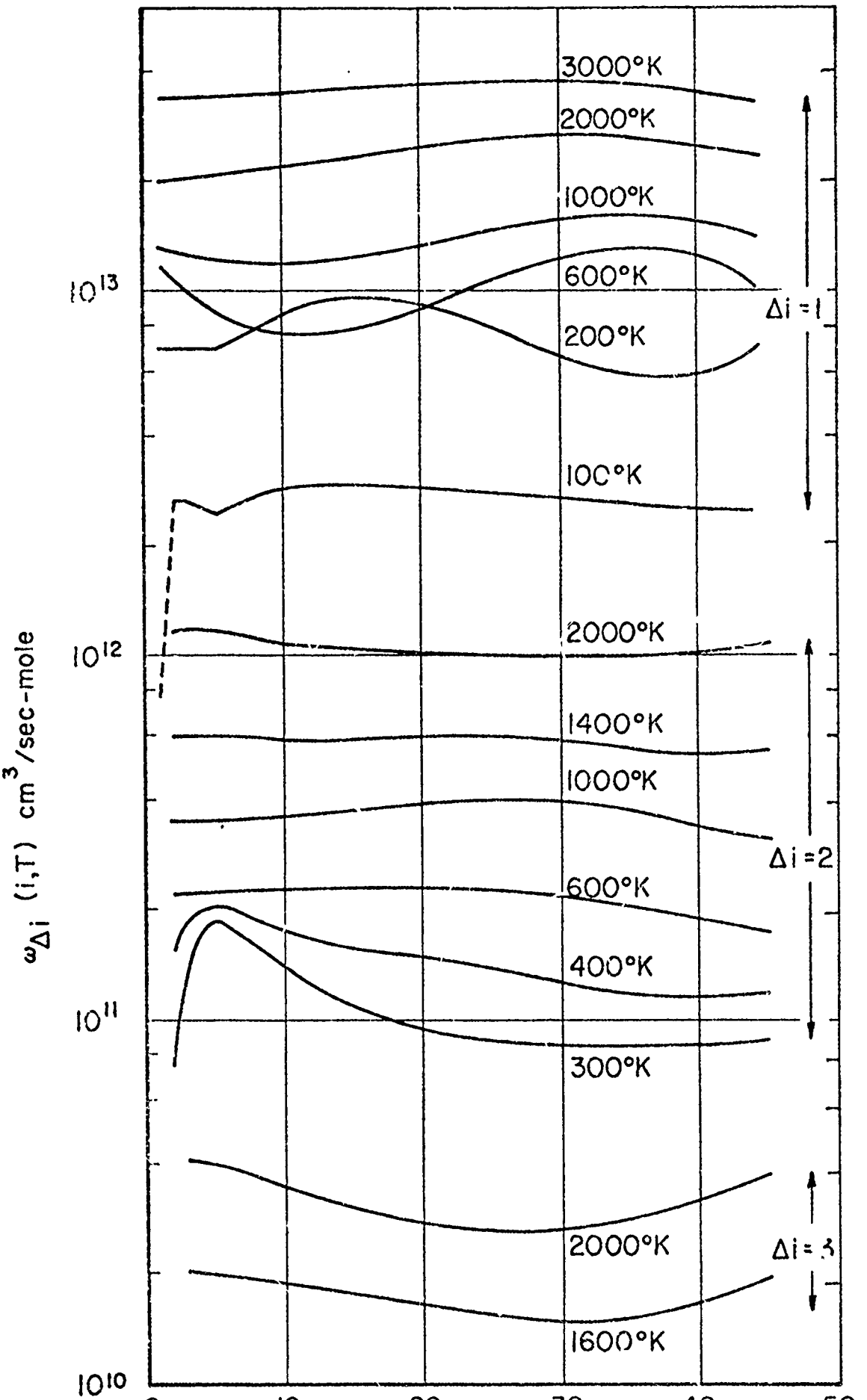
3000°K
2000°K
1000°K
600°K
200°K
100°K
2000°K
1400°K
1000°K
600°K
400°K
300°K
2000°K
1600°K
Δi = 1
Δi = 2
Δi = 3
10^{13}
10^{12}
10^{11}
10^{10}
$\omega_{\Delta i}$ (i,T) cm^3/sec-mole
0
10
20
30
40
50
i

Fig 1.

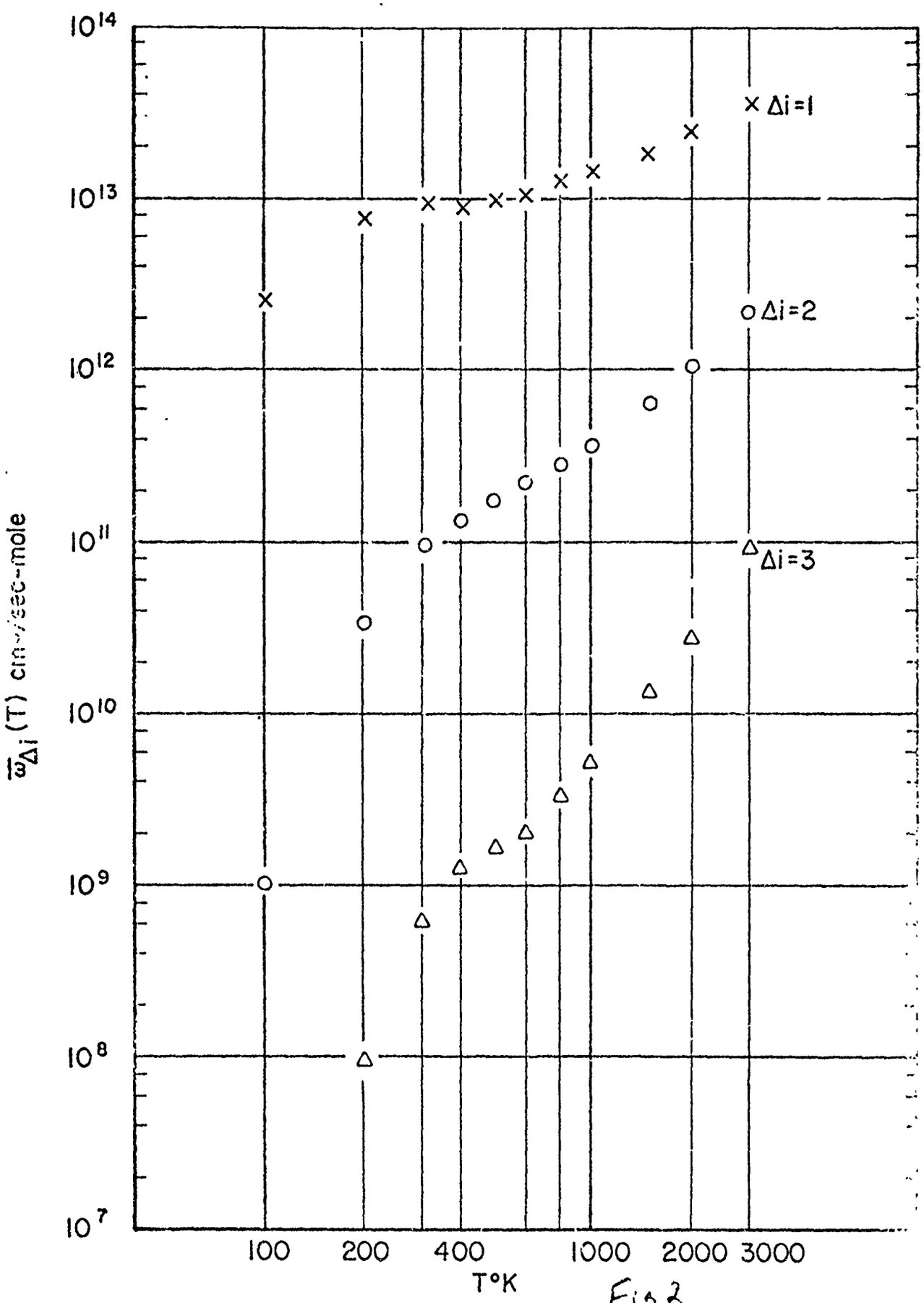
10^{14}
10^{13}
10^{12}
10^{11}
10^{10}
10^{9}
10^{8}
10^{7}
$\bar{\omega}_{\Delta i}(T)$ cm⁻¹/sec-mole
× Δi=1
○ Δi=2
△ Δi=3
100
200
400
1000
2000
3000
T°K

Fig 2

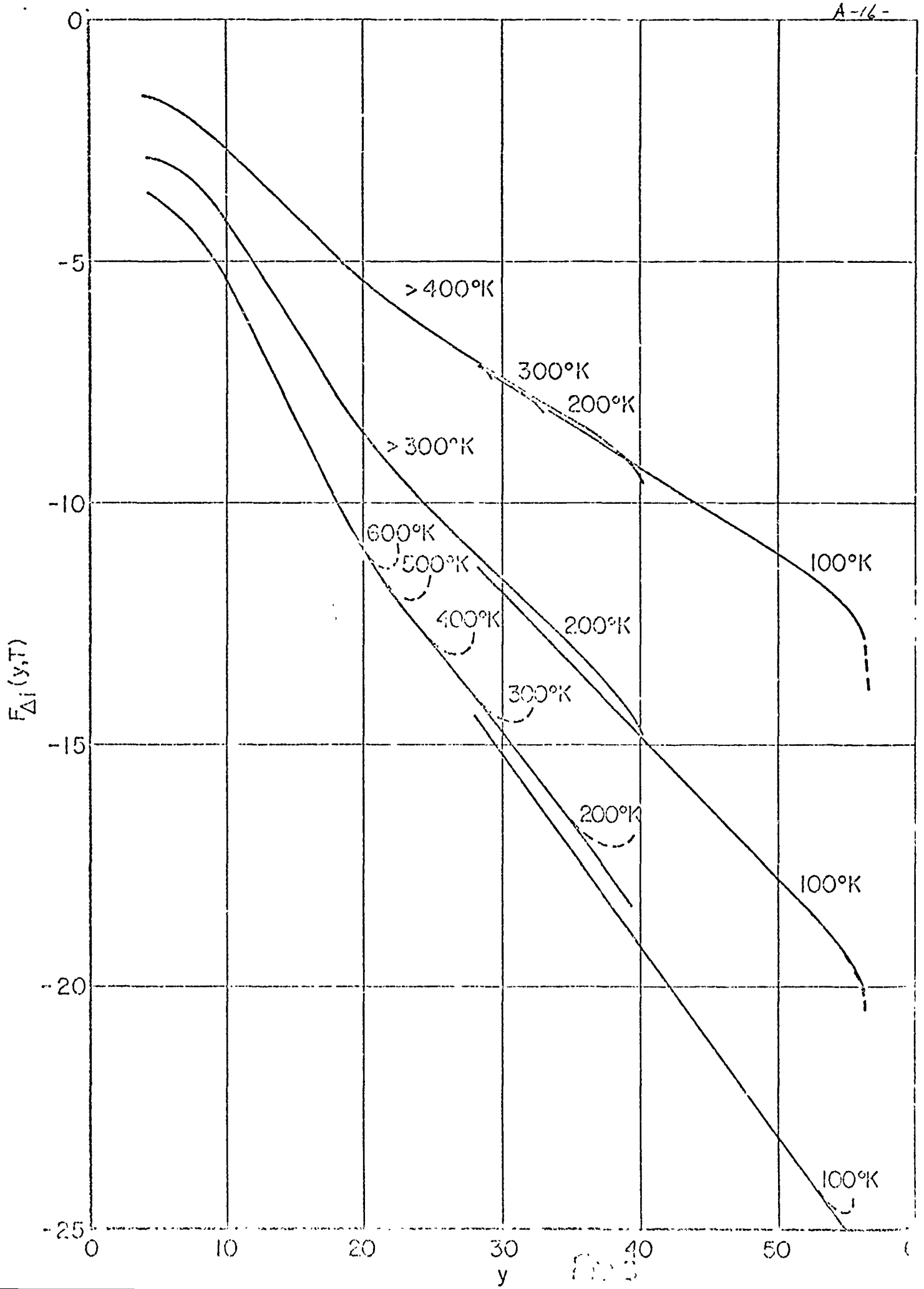
0
-5
-10
-15
-20
-25
0
10
20
30
40
50
y
$F_{\Delta i}(y,T)$
>400°K
300°K
200°K
>300°K
600°K
500°K
400°K
300°K
200°K
100°K
200°K
100°K
100°K

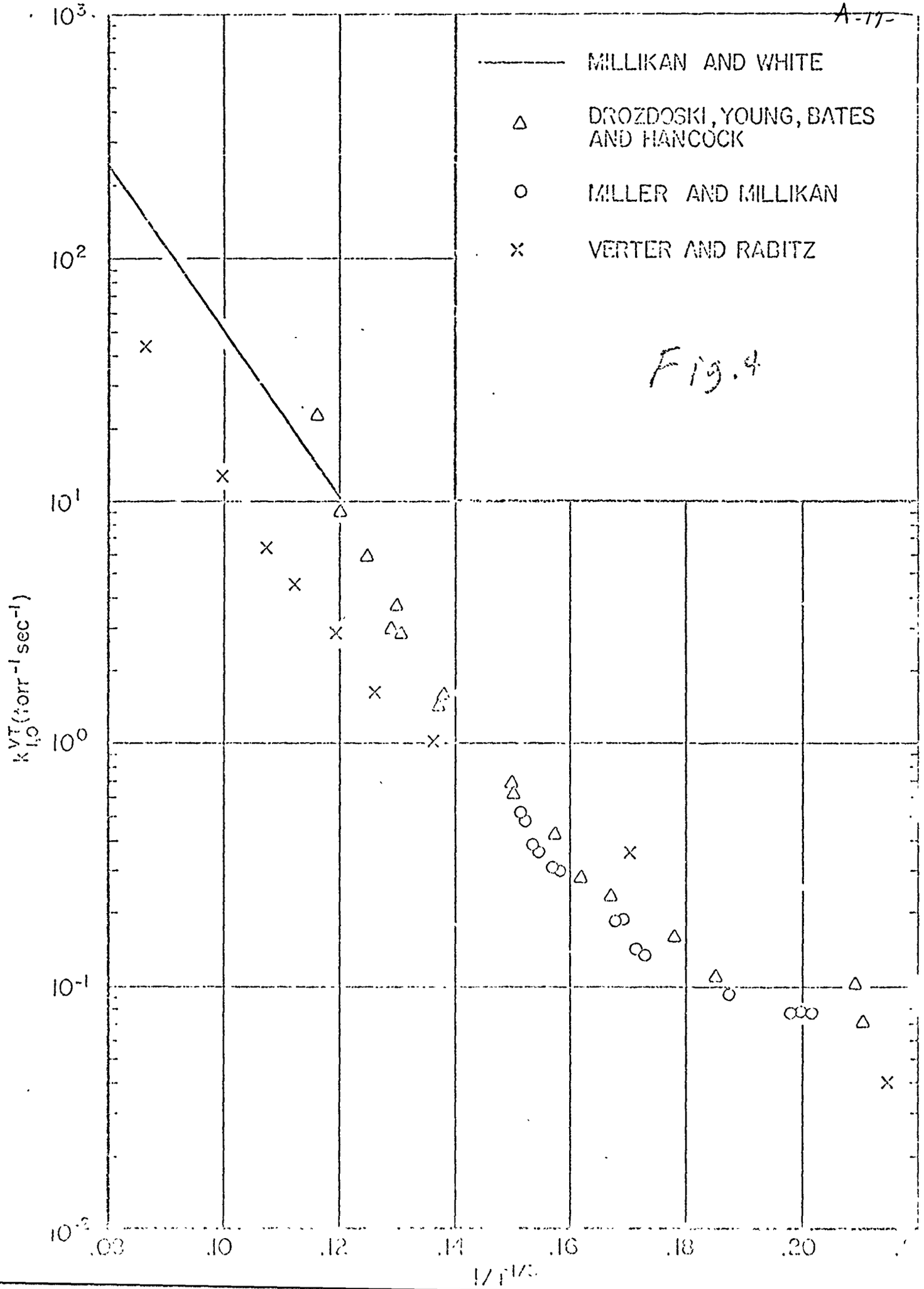
MILLIKAN AND WHITE
DROZDOSKI, YOUNG, BATES AND HANCOCK
MILLER AND MILLIKAN
VERTER AND RABITZ
10^3
10^2
10^1
10^0
10^{-1}
10^{-2}
$k_{1,0}^{VT}$(torr^{-1}sec^{-1})
.08
.10
.12
.14
.16
.18
.20
$1/T^{1/3}$

Fig. 4

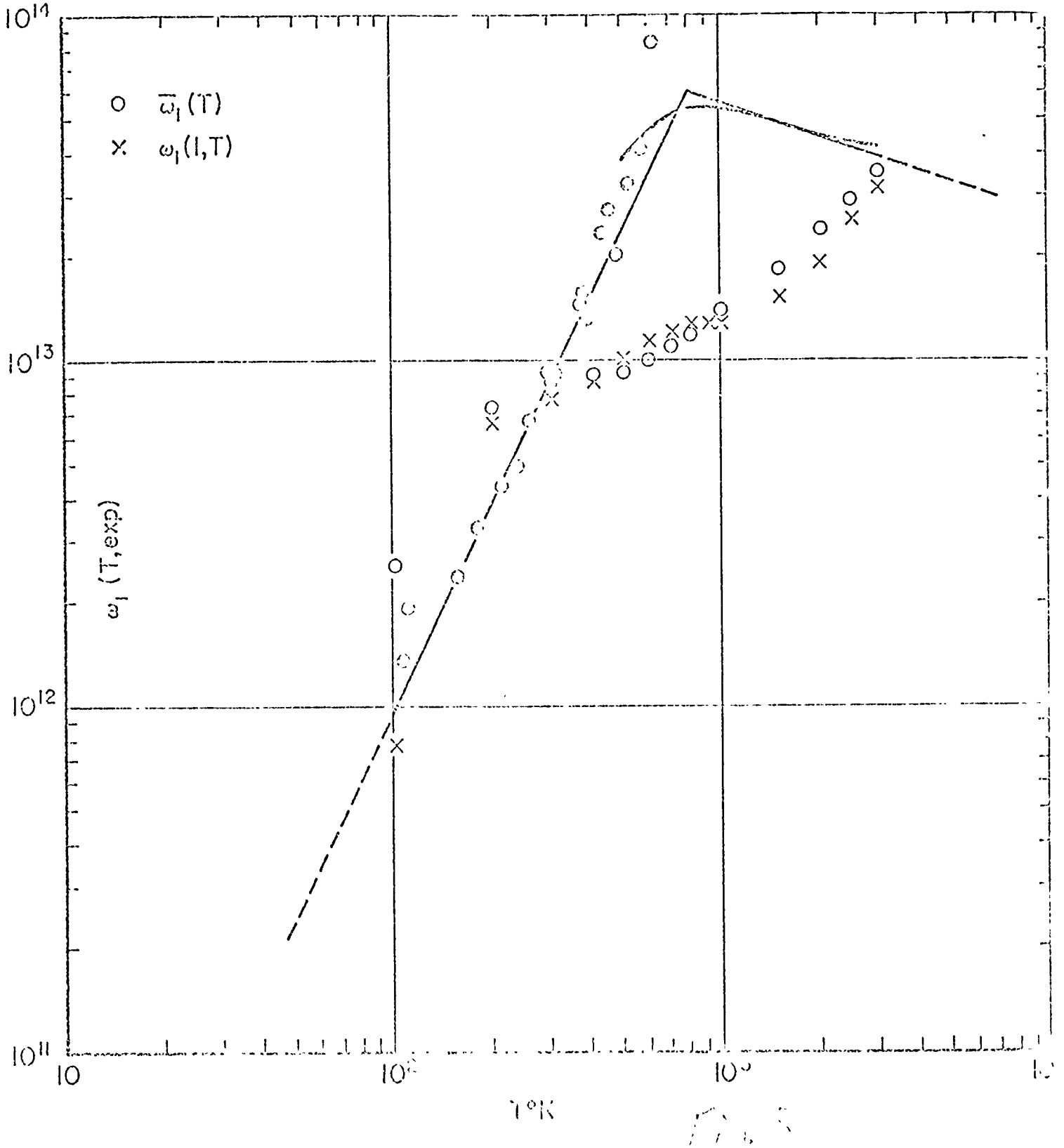
10^{14}
10^{13}
10^{12}
10^{11}
$\bar{\omega}_1(T)$
$\omega_1(I,T)$
$\omega_1(T,exp)$
10
T°K

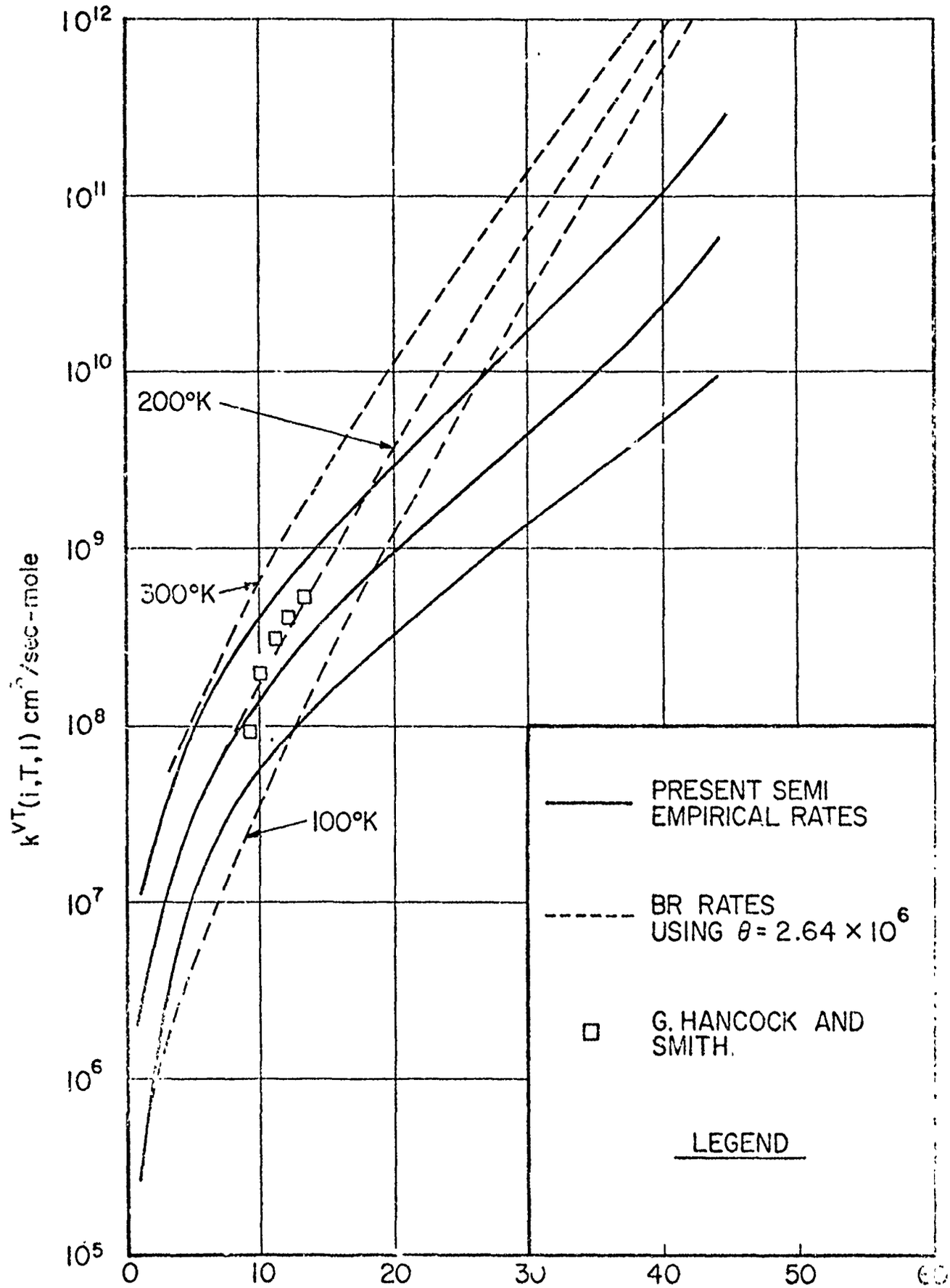
10^{12}
10^{11}
10^{10}
10^{9}
10^{8}
10^{7}
10^{6}
10^{5}
$k^{VT}(i,T,1)$ cm^3/sec-mole
200°K
300°K
100°K
PRESENT SEMI EMPIRICAL RATES
BR RATES USING $\theta = 2.64 \times 10^6$
G. HANCOCK AND SMITH.
LEGEND
0
10
20
30
40
50
60
i

Fig. 6

VIBRATION-ROTATION RELAXATION IN BIMOLECULAR COLLISIONS WITH APPLICATION TO PARA-HYDROGEN

by

Ramakrishna Ramaswamy

and

Hersch I Rabitz*

Department of Chemistry

Princeton University

Princeton, New Jersey 08540

ABSTRACT

Three-dimensional quantum mechanical calculations in the effective potential approximation have been made on the para-hydrogen system. At low temperatures vib-rotationally inelastic collisions were examined while breathing sphere calculations were used to probe the high-temperature regime. It was found that simultaneous vibrational and rotational processes contribute to the overall mechanism of vibrational relaxation. Both intra- and intermolecular energy transfer is possible in the present calculation, and the corresponding cross sections are examined in detail. Rates are calculated from the cross sections and compared with experiment.

I. INTRODUCTION

Processes involving energy transfer in bimolecular collisions are frequently categorized as rotation-translation (R-T), vibration-translation (V-T), vibration-vibration (V-V) and vibration-rotation-translation (V-R-T). A study of a system of gaseous molecules must, if it is to be complete, focus simultaneously on all these modes of energy transfer. It is also most desirable to treat the problem within a quantum mechanical framework. Vibrational excitation and de-excitation in collisions is an important process in gas laser systems and relaxation phenomena.[1] Research on the contributing physical factors in such energy transfer is desirable. Understanding the role of rotational inelasticity accompanying the vibrational inelasticity is also believed crucial in interpreting some relaxation phenomena. The analysis of the scattering properties of a system demands a reasonably accurate knowledge of the interaction potential in order to properly reproduce the dynamics. As a practical matter, the computational expense must remain within a reasonable limit if detailed analysis is to be possible.

In this context, the para-hydrogen system is an attractive one with a view to examining the processes mentioned above. A study of hydrogen is useful in itself and may provide a model for more complex systems. The purely vibrational problem has been approached in the distorted wave formalism by Calvert,[2a] who calculated the ratio of de-excitation rates for H_2-H_2 and H_2-D_2. A collinear study of near resonant V-V processes H_2-D_2 collisions was made by Alexander[2b] using a variety of intermolecular potentials, including the one used in this study. More recently rotations and vibrations have been included in a three-dimensional semiclassical study by Fisher and Billing.[2c] We have chosen to solve the quantum scattering equations for this system in

the effective potential (EP) approximation.[3a] With this approach the dimensionality of the coupled equations that must be solved is greatly reduced in comparison to the exact-close-coupled equations.[3b] In this fashion the large numbers of channels involved in a vibrotational calculation can be manageably handled. The shock tube experiments of Kiefer and Lutz[4] and Dove and Teitelbaum[5] as well as the low-temperature stimulated Raman scattering experiments of Ducuing et al.[6] for H_2 allow a comparison with some of the calculations.

We have examined the para-H_2 – para-H_2 collision from two points of view. Firstly, the molecules are treated as two breathing spheres (i.e., they are restricted to the rotational state $J = 0$). In the second case the coupled vibration-rotation equations are solved in the EP approximation; the effect of including rotational sub-levels on the ground and first excited vibrational levels was then studied. This latter work serves to complement the partial pictures of purely rotational and breathing sphere calculations.

Section II reviews the theoretical framework pertinent to this work. In Section III the intermolecular potential is discussed. Sections IV and V examine the cross section and rate behavior of the V-T and V-V and V-R-T processes as well as the associated relaxation phenomena. The final Section VI draws conclusions from the study.

II. THEORETICAL FRAMEWORK

The EP approximation[3] has been extensively discussed earlier, both with regard to theoretical development[7] and practical validity.[8] The formulation[7,9] is extended to the case of two identical vib-rotors in the present treatment.

The Hamiltonian of this system is

$$H = T + H_0(\text{int}) + V \tag{1}$$

where T is the kinetic energy operator, V the interaction potential, and $H_0(\text{int})$ the unperturbed vib-rotational Hamiltonian operator of the colliding molecules. Effective eigenstates of $H_0(\text{int})$ are written as $|n_1 j_1 n_2 j_2\rangle$, with $n_i j_i$ describing the vibrational and rotational quantum states of molecule $i = 1,2$. The interaction potential V is usually expanded in a sum of spherical harmonics over the orientation of angles of the two molecules

$$V(\vec{r}_1,\vec{r}_2,\vec{R}) = \sum_{\ell_1\ell_2\ell} \sum_{m_1 m_2 m} A_{\ell_1\ell_2\ell}(r_1 r_2 R)\langle \ell_1 m_1 \ell_2 m_2 | \ell_1 \ell_2 \ell m\rangle$$

$$Y_{\ell_1 m_1}(\hat{r}_1)\, Y_{\ell_2 m_2}(\hat{r}_2)\, Y^*_{\ell m}(\hat{R}) \tag{2}$$

where $A_{\ell_1\ell_2\ell}$ are the expansion coefficients, $\vec{r}_1$ and $\vec{r}_2$ define the vibrational coordinates of the two molecules in the space-fixed coordinate system, and $\vec{R}$ is the vector joining the centers of mass of the two molecules. This expression is considerably simplified in the body-fixed axes[8b] shown in Fig. 1. Further discussion of the potential is contained in Section III below.

The effective potential[10] matrix elements are given by

$$\langle n_1 j_1 n_2 j_2 | V^{eff}(R) | n_1' j_1' n_2' j_2' \rangle = N_0 \exp(i\eta)$$

$$\sum_{\ell_1 \ell_2 \ell} \langle n_1 n_2 | A_{\ell_1 \ell_2 \ell}(R) | n_1' n_2' \rangle \langle j_1 j_2 \| T_{\ell_1 \ell_2 \ell} \| j_1' j_2' \rangle \qquad (3)$$

where

$$N_0 = \left([j_1][j_2][j_1'][j_2'] \right)^{-1/4}$$

$$\eta = \left\{ | j_1 + j_2 - j_1' - j_2' | + j_1' + j_2' + j_1 + j_2 \right\} \frac{\pi}{2}$$

$$\langle j_1 j_2 \| T_{\ell_1 \ell_2 \ell} \| j_1' j_2' \rangle = \left[\frac{[j_1][j_2][j_1'][j_2'][\ell]}{(4\pi)^3} \right]^{1/2} \begin{pmatrix} j_1 & \ell_1 & j_1' \\ 0 & 0 & 0 \end{pmatrix} \begin{pmatrix} j_2 & \ell_2 & j_2' \\ 0 & 0 & 0 \end{pmatrix}$$

$[k] = 2k+1$, and $(:::)$ is a 3-J symbol.[11]

The expansion coefficients have been integrated over the vibrational coordinates with respect to the vibrational states, $\langle r | n_i \rangle = \varphi_{n_i}(r)$

$$n_1 n_2 | A_{\ell_1 \ell_2 \ell}(R) | n_1' n_2' \rangle = \int\int dr_1 dr_2 \, \varphi^*_{n_1}(r_1) \, \varphi^*_{n_2}(r_2) \, A_{\ell_1 \ell_2 \ell}(r_1 r_2 R) \, \varphi_{n_1'}(r_1) \, \varphi_{n_2'}(r_2) \qquad (4)$$

Equation (4) assumes separability of the molecular vibration-rotation wavefunctions; this approximation can easily be relaxed if necessary.

In the case of homonuclear diatomics the additional symmetry under nuclear interchange requires that the total wavefunction be symmetric. The

observed cross section, σ^{obs}, is a statistically weighted sum of symmetrized cross sections

$$\sigma^{obs} = \sigma^{+} W^{s} + \sigma^{-} W^{a} \qquad (5)$$

where the + and - signs refer to the total symmetry of the spatial part of the wavefunction. For hydrogen, which is a boson, these weights are given by

$$W^{s} = \frac{I+1}{2I+1}, \qquad W^{a} = \frac{I}{2I+1},$$

where I is the total nuclear spin (0 for para-H_2).
The wavefunction is then expanded in a symmetrized basis set,

$$I^{\pm}_{\ell n_1 j_1 n_2 j_2}(1,2|\theta) =$$

$$\left[2\left(1+\delta_{n_1 n_2}\delta_{j_1 j_2}\right)\right]^{-1/2} \left\{\varphi_{n_1 j_1}(1)\,\varphi_{n_2 j_2}(2) \pm (-1)^{\ell}\varphi_{n_1 j_1}(2)\varphi_{n_2 j_2}(1)\right\} P_{\ell}(\cos\theta) \qquad (6)$$

where θ is the polar angle of $\vec{R}$. This results in the following form for the symmetrized wavefunction

$$\psi^{\pm}(R,1,2) = \frac{1}{R}\sum U^{\pm}_{\ell n_1 j_1 n_2 j_2}(R)\; I^{\pm}_{\ell n_1 j_1 n_2 j_2}(1,2|\theta) \qquad (7)$$

where the sum is over all the indices. In this basis set the symmetrized EP matrix elements become

$$\langle \ell n_1 j_1 n_2 j_2 | V^{\pm(\mathrm{eff})}(R) | \ell' n_1' j_1' n_2' j_2' \rangle =$$

$$\delta_{\ell\ell'} \left\{ \left(1+\delta_{n_1 n_2} \delta_{j_1 j_2}\right) \left(1+\delta_{n_1' n_2'} \delta_{j_1' j_2'}\right) \right\}^{-1/2}$$

$$\times \left\{ \langle n_1 j_1 n_2 j_2 | V^{\mathrm{eff}}(R) | n_1' j_1' n_2' j_2' \rangle \pm (-1)^{\ell} \langle n_1 j_1 n_2 j_2 | V^{\mathrm{eff}} | n_2' j_2' n_1' j_1' \rangle \right\} \qquad (8)$$

The coupled differential equations for the system are then

$$\left[-\frac{\hbar^2}{2\mu} \left\{ \frac{d^2}{dR^2} - \frac{\ell(\ell+1)}{R^2} \right\} + E_{n_1 j_1} + E_{n_2 j_2} - E \right] U^{\pm}_{\ell n_1 j_1 n_2 j_2}(R) =$$

$$- \sum_{n_1' j_1' n_2' j_2'} \langle \ell n_1 j_1 n_2 j_2 | V^{\pm \mathrm{eff}} | \ell n_1' j_1' n_2' j_2' \rangle U^{\pm}_{\ell n_1' j_1' n_2' j_2'}(R) \qquad (9)$$

where μ is the reduced mass of the colliding pair, $E_{n_i j_i}$ are the internal energies of the molecules $i = 1,2$, and E is the total energy at which the molecules collide. The ground state of each molecule E_{00} is the zero point energy, 0.268 eV, and the total energy satisfies the relation $E \geq 2E_{00}$. The asymptotic solution to the Eqs. (8) yields the scattering amplitude from which the symmetrized $S^{\pm}$ matrix may be obtained

$$U^{\pm}_{\ell n_1 j_1 n_2 j_2}(R) \sim \left(\frac{1}{2\pi}\right)^{3/2} \left[\delta_{n_1 n_1'} \delta_{n_2 n_2'} \delta_{j_1 j_1'} \delta_{j_2 j_2'} \exp\left(i k_{n_1 j_1 n_2 j_2} R \cos\theta\right) \right.$$

$$\left. \pm \delta_{n_1 n_2'} \delta_{n_2 n_1'} \delta_{j_2 j_1'} \delta_{j_1 j_2'} \exp\left(i k_{n_1 j_1 n_2 j_2} R \cos(\pi - \theta)\right) \right]$$

$$+ \frac{1}{R} \exp\left(i k_{n_1' j_1' n_2' j_2'} R\right) \left\{ f(n_1 j_1 n_2 j_2 \to n_1' j_1' n_2' j_2' | \theta) \pm f(n_1 j_1 n_2 j_2 \to n_2' j_2' n_1' j_1' | \pi - \theta) \right\}$$

(10)

where $k_{n_1 j_1 n_2 j_2}$ is a wave vector. The symmetrized scattering amplitude may be defined as

$$f^{\pm}(n_1 j_1 n_2 j_2 \to n_1' j_1' n_2' j_2' | \theta) = f(n_1 j_1 n_2 j_2 \to n_1' j_1' n_2' j_2' | \theta)$$

$$\pm f(n_1 j_1 n_2 j_2 \to n_2' j_2' n_1' j_1' | \pi - \theta)$$

$$= \left(-2i\sqrt{k_{n_1 j_1 n_2 j_2}\, k_{n_1' j_1' n_2' j_2'}}\right)^{-1}$$

$$\times \sum_{\ell=0}^{\infty} (2\ell+1)\left[\left(1 \pm (-1)^{\ell} \delta_{n_1 n_2} \delta_{j_1 j_2}\right)\left(1 \pm (-1)^{\ell} \delta_{n_1' n_2'} \delta_{j_1' j_2'}\right)\right]^{1/2}$$

$$\times \left[\delta_{n_1 n_1'} \delta_{n_2 n_2'} \delta_{j_1 j_1'} \delta_{j_2 j_2'} - S_{\ell}^{\pm}(n_1 j_1 n_2 j_2 ; n_1' j_1' n_2' j_2')\right] P_{\ell}(\cos\theta) \qquad (11)$$

The total cross section is then given by

$$\sigma^{\pm}(n_1 j_1 n_2 j_2 \to n_1' j_1' n_2' j_2') = \frac{\pi}{k^2_{n_1 j_1 n_2 j_2}} \left[\frac{[j_1'][j_2']}{[j_1][j_2]}\right]^{1/2}$$

$$\sum_{\ell=0}^{\infty} (2\ell+1)\left[1 \pm (-1)^{\ell} \delta_{n_1 n_2} \delta_{j_1 j_2}\right]\left[1 \pm (-1)^{\ell} \delta_{n_1' n_2'} \delta_{j_1' j_2'}\right]$$

$$\times \left|\delta_{n_1 n_1'} \delta_{j_1 j_1'} \delta_{n_2 n_2'} \delta_{j_2 j_2'} - S_{\ell}^{\pm}(n_1 j_1 n_2 j_2 ; n_1' j_1' n_2' j_2')\right|^2 \qquad (12)$$

The above results can readily be applied to the case of two breathing spheres by setting $j_1 = j_2 = j_1' = j_2' = 0$ and retaining only the term $\ell_1 = \ell_2 = \ell = 0$ in the potential in Eq. (3).

After generating total cross sections σ^{obs} as a function of kinetic energy, rates of excitation and de-excitation can be obtained as a function of temperature by averaging over the kinetic energy.[12] The appropriate excitation rate constant is given by the expression

$$k_{i\to j}(T) = \left(\frac{2}{KT}\right)^{3/2}\left(\frac{1}{\mu\pi}\right)^{1/2} \exp\left((E_i - E_j)/KT\right) \int_0^\infty (\epsilon + E_j - E_i)\sigma_{i\to j}(\epsilon + E_j)\exp(-\epsilon/KT)d\epsilon \tag{13}$$

where $E_j \geq E_i$ and $\epsilon = E - E_j$ is the final kinetic energy. The abbreviated indices i,j label the molecular levels and K is Boltzmann's constant. In a similar fashion, for de-excitation $(E_j > E_i)$, the expression becomes

$$k_{j\to i}(T) = \left(\frac{2}{KT}\right)^{3/2}\left(\frac{1}{\mu\pi}\right)^{1/2} \int_0^\infty \epsilon\sigma_{j\to i}(\epsilon+E_j)\exp(-\epsilon/KT)\,d\epsilon \tag{14}$$

Equations (13) and (14) are related by detailed balance and in this paper the units of k(T) are $cm^3\ sec^{-1}\ molecule^{-1}$. The various equations developed in this section will be applied in Sections IV, V and VI.

III. THE INTERMOLECULAR POTENTIAL

The interaction potential between two hydrogen molecules has been discussed in some detail in the literature,[13] and much work is still proceeding.[14] Unfortunately for our purposes most potentials developed thus far are unsuitable for application in a study of vibrations since they examine the H_2-H_2 surface keeping the intramolecular H-H bond distance at the equilibrium value of ~ 1.4 Bohr. Since the effective potential matrix elements in Eq. (3) must be obtained by integrating over the vibrational coordinates in Eq. (4), the potential surface must be known as a function of these coordinates. Currently the only available potentials that incorporate this feature are the Silver-Karplus London[13f] and Valence-Bond (VB) surfaces.[13g] As was demonstrated elsewhere,[15] the inherent simplicity of the latter surfaces precludes a high degree of accuracy. However, these surfaces are believed to be qualitatively correct,[13f] and they should allow for a determination of the basic physical effects dominating the collision. This goal is in accord with the purpose of this research, which is the determination of the collisional mechanism that is operative in hydrogen relaxation.

The potentials were generated as a function of the angles θ_1, θ_2, and $(\varphi_1 - \varphi_2)$, and the distances r_1, r_2 and R. They were then fit by a least squares procedure[16] to the expansion in spherical harmonics in Eq. (2), including all terms up to A_{224}. This expansion incorporates the principal components of the potential: the spherical term A_{000} and the various short- and long-range anisotropies A_{202}, A_{022} and A_{224}. In computing the coupling matrix elements, the H_2 molecule was treated as a Morse oscillator,[17] and the integration in Eq. (4) performed numerically.

A few additional comments are necessary concerning the potential. As the H_2 molecule is stretched to a bond distance greater than 3 Bohr, the potential becomes decidedly more anisotropic than can be adequately expressed by a least squares fit to the six-term expansion employed above. The number of vibrational states n that can be included is therefore limited to those whose wavefunctions $\varphi_n(r)$ die out sufficiently by $r = 3$ Bohrs. This is not a severe restriction since the basic trends are discernible within this framework.

IV. COMPUTATION OF CROSS SECTIONS

A. General Comments

The Gordon algorithm[18] was used in solving the coupled scattering equations, Eq. (10). The utilization of symmetrized basis states in Eq. (7) requires solving fewer coupled equations. This procedure also results in the calculation of $\sigma^{\pm}$

$$\sigma^{\pm}(n_1 j_1 n_2 j_2 \rightarrow n_1' j_1' n_2' j_2') = \sigma(n_1 j_1 n_2 j_2 \rightarrow n_1' j_1' n_2' j_2') \pm \sigma(n_1 j_1 n_2 j_2 \rightarrow n_2' j_2' n_1' j_1') \quad (15)$$

which is an inseparable sum/difference of direct and exchange cross sections respectively (neglecting the generally weak interference terms). Note that for para-H_2 the statistical weight, $W^a = 0$, and only S_ℓ^+ matrices need be calculated to obtain σ^{obs} on Eq. (5). In actual computations the basis set used in calculating even or odd ℓ valued S_ℓ^+ matrices is different because of the nature of the symmetrized potential matrix in Eq. (8). The S_ℓ^+ matrices corresponding to even or odd ℓ values behave similarly as a function of ℓ, but they can have differing contributions to the total cross section. Within either set, however, it is often sufficient to compute the matrices at a uniformly spaced grid (rather than each ℓ value) since the behavior is smooth as a function of ℓ.

The total energies of the calculation were on the range $1.05 \text{ eV} \leq E \leq 3.12$ for the case of two breathing spheres and $0.5 \text{ eV} \leq E \leq 1.35 \text{ eV}$ for two vibrotors Since vibrationally excited states are closed below 1.05 eV, only purely rotational information is obtained in the lower regime. A more thorough treatment of this aspect is to be presented elsewhere,[15] and only brief comments concerning pure rotations will be made below. Vibrational transitions

inherently lead to extremely small cross sections (save the near-resonant V-V cases) particularly near thresholds. The difficulties of calculation in these cases have been discussed elsewhere,[19] and one must use tight tolerances.[18] Nevertheless, a certain degree of "noise" still enters, and we have found it expedient, with the rate calculations of the following section in mind, to smooth them using a spline fit.[20]

B. Breathing Sphere Transitions

The maximum basis set employed in these calculations, in the notation $n_1 n_2$, is shown in Fig.2(a) The actual basis set in any particular calculation depended on the number of states open at that energy. The $S_\ell^\pm$ matrices were tested for basis set convergence and at varying tolerances to ensure numerical stability. It was generally necessary to include two closed channels for convergence.

Due to differences in the two potentials used, especially in their slopes at small intermolecular separations, cross sections for the various inelastic transitions can sometimes differ by an order of magnitude.[2b] The steeper slope of the VB potential gives rise to larger cross sections. However, the behavioral aspects of the cross sections from the two potentials are quite similar. In particular, transitions involving the change of the same number of quanta are grouped together and are generally separated from other groups by approximately an order of magnitude. This is illustrated in Fig.3(a)which shows the results of calculations using the VB potential. Each band encompasses the de-excitation cross sections involving the same number of quanta, Δn, exchanged with translation

$$H_2(n_1,0) + H_2(n_2,0) \rightarrow H_2(n_1',0) + H_2(n_2',0)$$

$$\Delta n = (n_1 + n_2) - (n_1' + n_2')$$

The energy deficit, $\Delta E = E_{n_1 0} + E_{n_2 0} - E_{n_1' 0} - E_{n_2' 0}$, is different for the various transitions within each band, and this together with the different coupling effects accounts for the spread of the bands. Figure 3(b) and all following figures depict the results of calculations using the Vb potential since we feel that this potential is more in agreement qualitatively and quantitatively with the true physical potential (cf. Section VI below).

It is quite evident in Fig.3(a)that the near resonant V-V transitions, for which $\Delta n = 0$, have greatly enhanced cross sections and are well separated from those for which $\Delta n > 0$. The cross sections for $\Delta n > 0$ tend to overlap considerably in the threshold region. The individual cross sections generally rise with energy at different rates as shown in Fig.3(b)for a few typical cases. This behavior can give rise to different temperature scaling which will be discussed later.

The detailed behavior of the cross section in Fig.3(b)is rather complex, but some comments can be made. For instance, it is apparent that $\sigma_{03 \rightarrow 11} < \sigma_{03 \rightarrow 02}$ even though the energy transferred $\Delta E_{03 \rightarrow 11}$ is slightly smaller than $\Delta E_{03 \rightarrow 02}$. Both these transitions result in a net change of $\Delta n = 1$. However, physically these constitute different processes. Neglecting the weak exchange term, the case $03 \rightarrow 02$ corresponds to a change of one quantum on the second molecule, while $03 \rightarrow 11$ requires one molecule to gain a quantum and the other to lose two quanta. This latter case is clearly less

favorable due to diminished coupling effects. A similar situation occurs in the case of $\sigma_{02\to 00} > \sigma_{11\to 00}$. Caution is called for in any generalization of these results since it is apparent that $\sigma_{22\to 11} > \sigma_{22\to 02}$, at least at lower energies.

C. Vibration-Rotation Transitions

In the calculation of vibration-rotation S_ℓ^+ matrices by close coupling or even effective potential methods, the principal deterrent is the number of channels that must be included. While in the case of hydrogen this problem is reduced due to the large rotational spacing and weak coupling, even in this case the problem rapidly becomes serious. This is obvious in Fig.2(b)which shows the high density of the rotational states involved. In tackling a problem of this size, a certain judicious choice must be made concerning which states to include in order to achieve convergence of the desired S_ℓ^+ matrix elements. Another practical restriction is imposed through the time required per calculational step,[18] which is a function of the number of states.[21] In practice any basis larger than 20-25 states imposes excessive demands in terms of computer time. Calculation of each S_ℓ^+ matrix in the basis of Fig.2(b) took 8-10 minutes in double precision on an IBM 360/95 computer since the tolerances[18] had to be consistently maintained at 5×10^{-6}.

Tests of convergence were performed by varying the states in the basis. Purely rotational transition S_ℓ^+ matrix elements generally converged on inclusion of all states up to the energetically highest open level. Coupling decreases rapidly for large multi-quanta transitions, giving rise to extremely small cross sections for transitions like $0606 \to 0000$. Inclusion of such very high $0j_1 0j_2$ states did not affect the principal rotational and vibrational transitions.

The actual basis set, therefore, consisted of the twenty states shown in Fig.2(b)

Figure 4(a) shows several purely rotational cross sections as a function of energy. The principal ones, for which $\Delta j = 2$, lie mainly in the region 10^{-2} Å$^2 \leq \sigma \leq 10$ Å^2, and $\Delta j > 2$ cross sections decrease with increasing Δj. Figure 4(b) is a profile of de-excitation rotor transitions at a total energy of 1.06 eV. It is apparent that for inelastic rotational cross sections $\left(\sigma_{n_1 j_1 n_2 j_2 \rightarrow n_1 j_1' n_2 j_2'}\right)$ the largest member corresponds to $(j_1 + j_2) - (j_1' + j_2') = 2$. In addition, since the lower quantum states are energetically closer together, one readily sees for $j_1 < j_2$ that

$$\sigma_{j_1 j_2 \rightarrow j_1 - 2, j_2} > \sigma_{j_1 j_2 \rightarrow j_1 j_2 - 2}$$

Many of these trends were previously observed in atom-molecule collisions such as He-H_2 [8a] and in rigid-rotor studies on H_2-H_2.[9a] Although the trends are the same, the magnitudes of the previous H_2-H_2 cross sections[9a] based on a different potential are somewhat smaller. The same general behavior is seen for those transitions that involve one vibrationally excited molecule, with an additional interesting aspect that can be seen in the comparison of the two collisions

$$H_2(02) + H_2(00) \rightarrow H_2(00) + H_2(02) \qquad (a)$$

$$H_2(12) + H_2(00) \rightarrow H_2(10) + H_2(02) \qquad (b)$$

Case (a) is really an elastic collision due to the enormous contribution of the exchange term $\sigma(0200 \rightarrow 0200)$ in Eq. (15). In case (b) the exchange term is extremely small since the process would be a vibrational exchange. Therefore, case (b) must rely on the direct term $\sigma(1200 \rightarrow 1002)$ which itself describes an exchange of rotational quanta between the two molecules. The net result is that case (a) has a much larger cross section than case (b).

Figure 5 represents a typical profile of vibrotor de-excitation cross sections at a total energy of 1.2 eV. The transitions to the left of state 0100 on the abscissa are vibrotor cross sections, while pure rotor cross sections (neglecting the very weak exchange process) are to the right. It is directly visible that as the rotational quantum change Δj increases beyond 2, the cross sections decrease rapidly. This emphasizes the importance of coupling effects and shows the small magnitude of near resonant vibrotational sections which are necessarily accompanied by large changes of rotational quanta.

As can be expected, the largest cross sections are those for which $|\Delta j|$ is 0 or 2. The largest vibration-rotation (although not substantially) cross sections from 0010 and 0212 are to 0000 and 0202 respectively. Similarly the largest cross sections from 0210 and 0012 are to 0202 and 0000, respectively. These latter cases involve simultaneous vibrational and rotational transitions, while the former, purely vibrational. Some parallel observations on the $He-H_2$ system have been made recently.[21]

It must, however, be noted that the total energy of 1.2 eV in Fig. 5 is the same for all the cross sections. Hence the various cross sections are at different kinetic energies and this accounts for the generally low magnitude of transitions from level 0414 which is barely open at 1.2 eV.

For the comparable breathing sphere transition $\sigma^{BS}_{01\rightarrow 00}$ is slightly smaller than $\sigma^{VR}_{0100\rightarrow 0000}$ as has been observed in the He-H_2 system by Zarur and Rabitz.[8a] Recent work using the atom-breathing sphere model for the He-CO[22] and other model systems[23] has shown the approximation to give reasonable results under certain circumstances. Additional comments on this matter will be made in Section VI.

V. RATE AND RELAXATION BEHAVIOR

A. Breathing Sphere Rates

The rates were calculated from the cross sections by Eqs. (12) and (13) over a large range of temperatures. The rates are presented in Fig. 6 analogous to the cross sections in Fig.3(a). The behavior qualitatively follows that which can be deduced from the cross sections. However, it must be noted that differing threshold behavior gives rise to slightly different temperature dependence. At high temperatures the dependence is Landau-Teller while non-linear behavior on a $\log k(T)$ vs. $T^{-1/3}$ plot shows up below $\sim 600^0$ K.

The greatly enhanced rates for the near resonant V-V processes are a consequence of their extremely large cross sections in comparison to the $\Delta n > 0$ transitions. The VB potential indicates a difference between the rates for V-V and V-T processes of approximately a factor of 10^3-10^4. This is a very significant difference and it is not clear if the inclusion of rotational states would tend to diminish it.[2c,6b] Nevertheless, it is evident that ladder climbing mechanisms (i.e., transitions of the type $n_1 n_2 \rightarrow n_1 - 1, n_2 + 1$) are extremely important in the rapid and efficient transfer of population to higher vibrational levels.

Experimental measurements of the rate of self relaxation of vibrationally excited H_2 molecules by the simulated Raman scattering (SRS) method find no difference in the rates for ortho-or para-H_2 above 300^0 K.[6b] Below room temperature the para-H_2 – para-H_2 rate is slightly smaller than the ortho case. Figure 7 presents a comparison of the results of this calculation with both the SRS experiment (para-H_2) on the range 50^0-500^0 K and the shock tube data[4,5]

from 1000^0-3000^0 K (normal H_2). Of the two potentials used the results of the VB potential are closer to the experimental ones, which suggests that this is the more accurate one. The VB potential has been used in a collinear study of D_2-D_2 near resonant V-V processes by Alexander.[2b] In comparison with several ab initio potentials, it was observed that the VB potential gave smaller cross sections and this was attributed to the slow decrease of the potential at long range. While the agreement with experiment at high temperatures is substantially better than at low temperature, some discrepancy still exists. However, the breathing sphere rate behavior is at least qualitatively accurate.

B. Vibration-Rotation Relaxation

Rates were generated in a similar fashion for V-R-T transitions below 300^0 K. The restriction to this range was necessitated by the availability of only low energy cross sections. The results of these calculations are plotted in Fig. 7 in the following manner. First a rotationally summed de-excitation rate is defined by the relation

$$k^{tot}_{1j_1 0 j_2}(T) = \sum_{j_1' j_2'} k_{1j_1 0 j_2 \rightarrow 0 j_1' 0 j_2'}(T) \qquad (16)$$

These rates are shown in the inset of Fig. 7. The fact that rates from the states 0212, 0012 and 0210 are larger than that from 0010 is indicative of the importance of rotational transitions in vibrational excitation. Molecules in the states where j_1 and/or $j_2 \neq 0$ can apparently utilize different and stronger portions of the interaction potential.[9b]

Now consider the general V-R-T relaxation process between the ground and first excited vibrational states

$$H_2(1j_1) + H_2(0j_2) \rightleftharpoons H_2(0j_1') + H_2(0j_2')$$

The rate of change in the number density, ρ_{1j_1} of molecular species $H_2(1j_1)$ can be written as

$$\frac{d\rho_{1j_1}}{dt} = \sum_{j_2 j_1' j_2'} - k_{1j_1 0j_2 \rightarrow 0j_1' 0j_2'} \rho_{1j_1} \rho_{0j_2} + k_{0j_1' 0j_2' \rightarrow 1j_1 0j_2} \rho_{0j_1'} \rho_{0j_2'} \qquad (17)$$

Since rotational relaxation is generally much faster than vibrational relaxation, it is reasonable to assume that the rotational states form a Boltzmann distribution.[24] We may therefore write the number density as

$$\rho_{nj} = \rho_n P_{nj}$$

where

$$P_{nj} = \frac{(2j+1) \exp\left(-(E_{nj} - E_{no})/KT\right)}{\sum_{j'} (2j'+1) \exp\left(-(E_{nj'} - E_{no})/KT\right)} \qquad (18)$$

is the rotational population in vibrational level n. Substituting Eq. (18) in Eq. (17) and summing over j_1 leads to

$$\frac{d\rho_1}{dt} = \sum_{j_1} \frac{d\rho_{1j_1}}{dt} = \sum_{\text{all indices}} - k_{1j_1 0j_2 \rightarrow 0j_1' 0j_2'} \rho_1 P_{1j_1} \rho_0 P_{0j_2}$$

$$+ k_{0j_1' 0j_2' \rightarrow 1j_1 0j_2} \rho_0^2 P_{0j_1'} P_{0j_2'} \qquad (19)$$

Equation (19) naturally leads to a definition of the effective rate constant as

$$\bar{k}_{01 \rightarrow 00} = \sum_{j_1 j_2 j_1' j_2'} P_{1j_1} P_{0j_2} k_{1j_1 0j_2 \rightarrow 0j_1' 0j_2'} \qquad (20)$$

The effective vibrational equations governing the process are then

$$\frac{d\rho_0}{dt} = \bar{k}_{01 \rightarrow 00} \rho_0 \rho_1 - \bar{k}_{00 \rightarrow 01} \rho_0^2$$

$$\frac{d\rho_1}{dt} = - \frac{d\rho_0}{dt}$$

where the second equation is readily established.

This set of equations can be easily solved to yield

$$\frac{\rho_0(t)}{\rho} = \frac{\bar{k}_{01 \rightarrow 00} \rho_0(0)}{\left\{\left[\rho_0(0) \left\{\bar{k}_{01 \rightarrow 00} + \bar{k}_{00 \rightarrow 01}\right\}\right] + \left[\bar{k}_{01 \rightarrow 00} \rho - \rho_0(0) \left\{\bar{k}_{01 \rightarrow 00} + \bar{k}_{00 \rightarrow 01}\right\}\right] \times \exp\left(- \bar{k}_{01 \rightarrow 00} \rho t\right)\right\}}$$

where $\rho = \rho_0 + \rho_1$ is the total density.

It can readily be shown that as the system nears equilibrium $\left(\rho_0(0) \sim \rho_0(\infty) \text{ and } \rho_1(0) \sim \rho_1(\infty)\right)$, the above equations can be linearized to produce the following simple behavior

$$\rho_n(t) - \rho_n(\infty) = \left[\rho_n(\infty) - \rho_n(0)\right] \exp\left(-\rho_0(\infty)\, \lambda t\right)$$

for $n = 0,1$. The relaxation rate in the exponent under these conditions is the usual sum of up and down rates in a two-level system

$$\lambda = \bar{k}_{01 \to 00} + \bar{k}_{00 \to 01}$$

This relaxation rate is shown in Fig. 7 labeled vibrotor (with the VB potential). It is interesting to note that while the temperature dependences of $k^{tot}_{n_1 j_1 n_2 j_2}$ in the inset of Fig. 7 have mostly negative curvatures, the averaging procedure in Eq. (19) yields an overall rate with the normal positive curvature. The vibrotor calculation clearly lies closer to the experiment than the breathing sphere curves, but it still falls short of precise agreement.

VI. CONCLUSION

There seems to be little doubt that the essence of the relaxation mechanism is contained in the full vibrotor-vibrotor treatment with the VB potential. Further refinements are possible with more sophisticated potentials and perhaps improved dynamical methods. An important conclusion from the above analysis is that rotations do play a role in relaxation (at least in the low-temperature region examined in detail) and the artificial exclusion of $j \neq 0$ states in the breathing sphere approximation underestimates the efficacy of vibrationally active collisions. This is in accord with previous work on He-H_2 [8a] and the recent parallel semiclassical treatment of H_2-H_2.[2c] Clearly, rotational transitions would be expected to continue to enter into vibrational inelasticity at higher temperatures. However, this does not imply that the breathing sphere rates will have no region of applicability. In experiments such as those above[4,5,6b,c] the rotationally summed and averaged rates of Eq.(19) are the ones of relevance. The proper comparison is therefore between the breathing sphere rates and those of Eq.(19). Model calculations have shown that a region of applicability exists[23] for this approximation, depending on the nature of the interactions. Indeed in the case of He-CO[22,25] breathing sphere calculations were shown to be adequate. Further work is still needed on this important problem.

A few final comments are in order. These calculations are moderately expensive in terms of computer time required. It should be recalled that these were minimum size[3b] effective Hamiltonian calculations. It is therefore easy to grasp the magnitude of difficulty involved in studies of more complex (massive) molecules. Several ways of circumventing this problem can be suggested,[26] but it is beyond the scope of this paper to delve into this problem.

ACKNOWLEDGMENT

We thank Drs. P. Thaddeus and Sheldon Green for facilitating the computational aspects of this research. Appreciation is extended to Dr. David Silver for providing us with the potential surfaces used in these calculations. We acknowledge the partial support of this work by the Office of Naval Research and the Petroleum Research Fund administered by the American Chemical Society.

REFERENCES

* Camille and Henry Dreyfus Foundation Teacher-Scholar;
Alfred P. Sloan Foundation Research Fellow.

1. (a) M. J. Pilling, Sci. Prog. (Oxf.) 63, 397 (1976);
   (b) M. J. Berry, Ann. Rev. Phys. Chem. 26, 259 (1975);
   (c) E. Weitz and G. Flynn, Ann. Rev. Phys. Chem. 25, 275 (1974).
2. (a) J. B. Calvert, J. Chem. Phys. 56, 5071 (1972);
   (b) M. H. Alexander, J. Chem. Phys. 59, 6254 (1973);
   (c) E. Fisher and G. D. Billing, to be published.
3. (a) H. Rabitz, J. Chem. Phys. 57, 1718 (1972);
   (b) H. Rabitz, J. Chem. Phys. 63, 5208 (1975).
4. J. H. Kiefer and R. W. Lutz, J. Chem. Phys. 44, 658 (1966).
5. (a) J. E. Dove and H. Teitelbaum, Chem. Phys. 6, 431 (1974);
   (b) H. Teitelbaum, Thesis, University of Toronto, 1974.
6. (a) M.-M. Audibert, C. Joffrin, and J. Ducuing, Chem. Phys. Lett. 25, 158 (1974);
   (b) M.-M. Audibert, R. Vilaseca, J. Lukasik, and J. Ducuing, Chem. Phys. Lett. 31, 232 (1975);
   (c) M.-M. Audibert, Thesis, University of Paris - Sud, Orsay, 1976.
7. See H. Rabitz, "Effective Hamiltonians in Molecular Collisions," in Modern Theoretical Chemistry, Vol. III, W. H. Miller, Ed. (Plenum, 1976).
8. (a) H. Rabitz and G. Zarur, J. Chem. Phys. 61, 5076 (1974);
   (b) S. Green, J. Chem. Phys. 62, 2271 (1975).
9. (a) G. Zarur and H. Rabitz, J. Chem. Phys. 60, 2057 (1974);
   (b) See also Ref. 7.
10. Other effective potentials can also be found. See for example, S. Augustin and H. Rabitz, J. Chem. Phys. 64, 4821 (1976).

11. D. M. Brink and G. Satchler, Angular Momentum (Oxford University Press, 1975).

12. H. Rabitz and G. Zarur, J. Chem. Phys. 62, 1425 (1975).

13. (a) A. K. McMahan, H. Beck, and J. A. Krumhansl, Phys. Rev. A 9, 1852 (1974) and numerous references cited therein;

(b) E. Kochanski, Theor. Chim. Acta 39, 339 (1975);

(c) M. Urban and P. Hobza, Theor. Chim. Acta 36, 207, 215 (1975);

(d) R. D. Etters et al., Phys. Rev. A 12, 2199 (1975);

(e) J. C. Raich et al., J. Chem. Phys. 64, 5088 (1976);

(f) N. Brown and D. M. Silver, J. Chem. Phys. 65, 311 (1976);

(g) D. M. Silver and M. Karplus, private communication;

(h) N. Ostlund, to be published;

(i) G. A. Gallup, to be published.

14. (a) G. A. Gallup, private communication;

(b) N. Ostlund, private communication;
(c) W. Meyer, private communication.

15. R. Ramaswamy, S. Green, and H. Rabitz, to be published.

16. G. Forsythe, S.I.A.N.J. 3, 174 (1957).

17. P. M. Morse, Phys. Rev. 34, 57 (1929).

18. R. G. Gordon, Meth. Comp. Phys. 10, 81 (1971).

19. M. H. Alexander and P. McGuire, J. Chem. Phys. 64, 452 (1976).

20. C. Reinsch, Numer. Math. 10, 177 (1967).

21. (a) M. H. Alexander, Chem. Phys. Lett. 38, 417 (1976);

(b) M. H. Alexander and P. McGuire, Chem. Phys. 12, 31 (1976).

22. M. Verter and H. Rabitz, J. Chem. Phys. 64, 2939 (1976).

23. S. M. Tarr, J. Sampson, and H. Rabitz, J. Chem. Phys. 64, 5291 (1976).

24. For exceptions to this see Ref. 12.

25. J.-L. Boulnois, S. H. Lam, and H. Rabitz, to be published.

26. See the following paper for a possible approach, S. Augustin and H. Rabitz, J. Chem. Phys. 64, 1223 (1976).

FIGURE CAPTIONS

1. Body-fixed axes for the system of two molecules. $\vec{R}$ connects the centers of mass of the molecules and the six coordinates are R, r_1, r_2, θ_1, θ_2 and the dihedral angle $\varphi_1 - \varphi_2$.

2. (a) Energy spacing for the breathing sphere levels studied.
   (b) Energy spacing for the vibrotor levels considered.

3. (a) Breathing sphere deexcitation cross sections $\sigma(n_1n_2 \rightarrow n_1'n_2')$. Inset numbers denote the quanta lost to translation, $\Delta n = (n_1 + n_2) - (n_1' + n_2')$.
   (b) Selected cross sections between breathing sphere levels, $\sigma(n_1n_2 \rightarrow n_1'n_2')$.

4. (a) Selected rotor cross sections in both ground and excited vibrational levels.
   (b) Profile of rotor cross sections in the ground vibrational state at the total energy 1.06 eV. Lines connect the same initial state, $0j_1, 0j_2$.

5. Profile of various vibrotor cross sections at the same total energy 1.2 eV. Lines connect the same initial state $0j_1 1j_2$.

6. Deexcitation rates for H_2 breathing spheres. Bands encompass rates for transitions involving the same number of quanta lost to translation, $\Delta n = (n_1 + n_2) - (n_1' + n_2')$.

7. Rates of deexcitation in para-H_2. Results of calculation with the London and VB potentials are compared with experiments. Vibrotor results are only presented for the VB potential. The inset shows low temperature summed rates defined in Eq. (16).

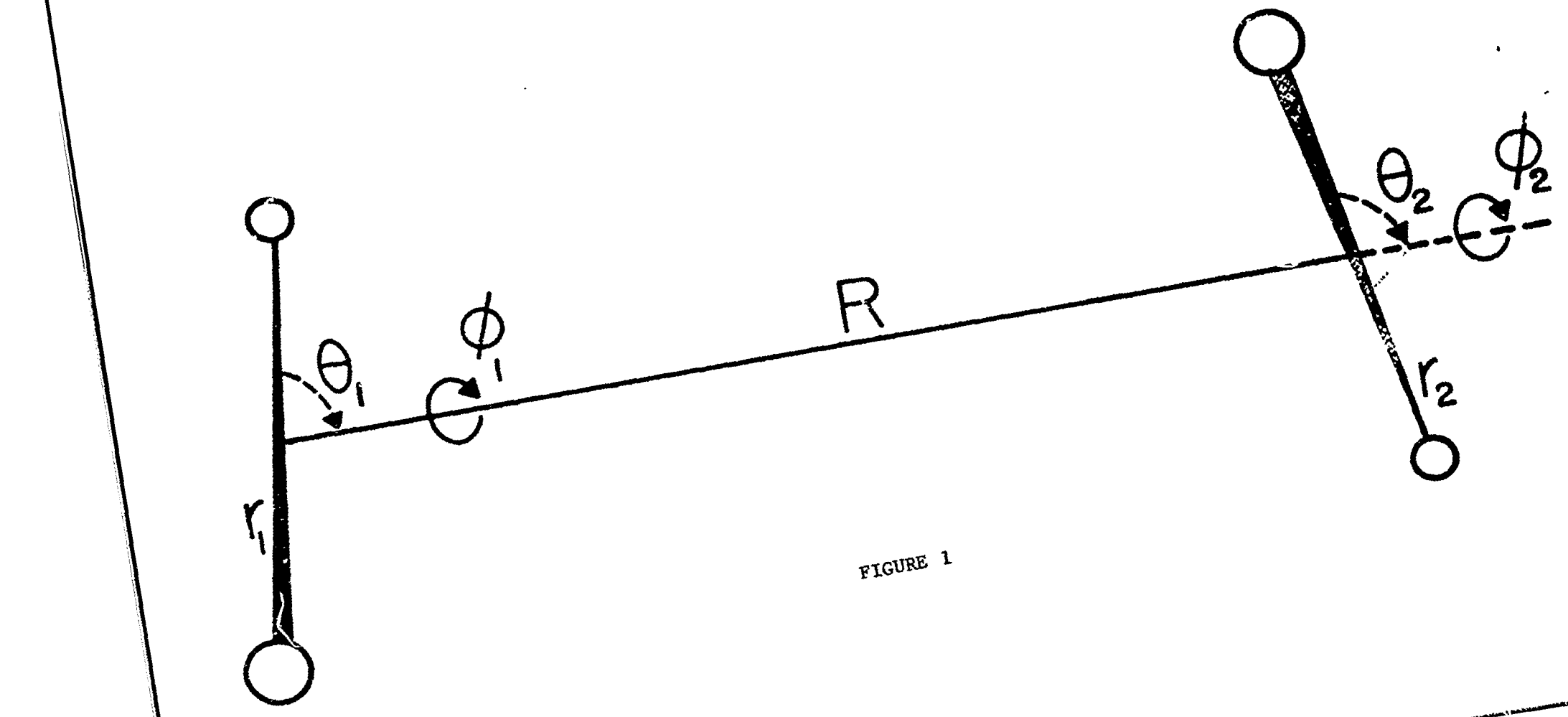

FIGURE 1

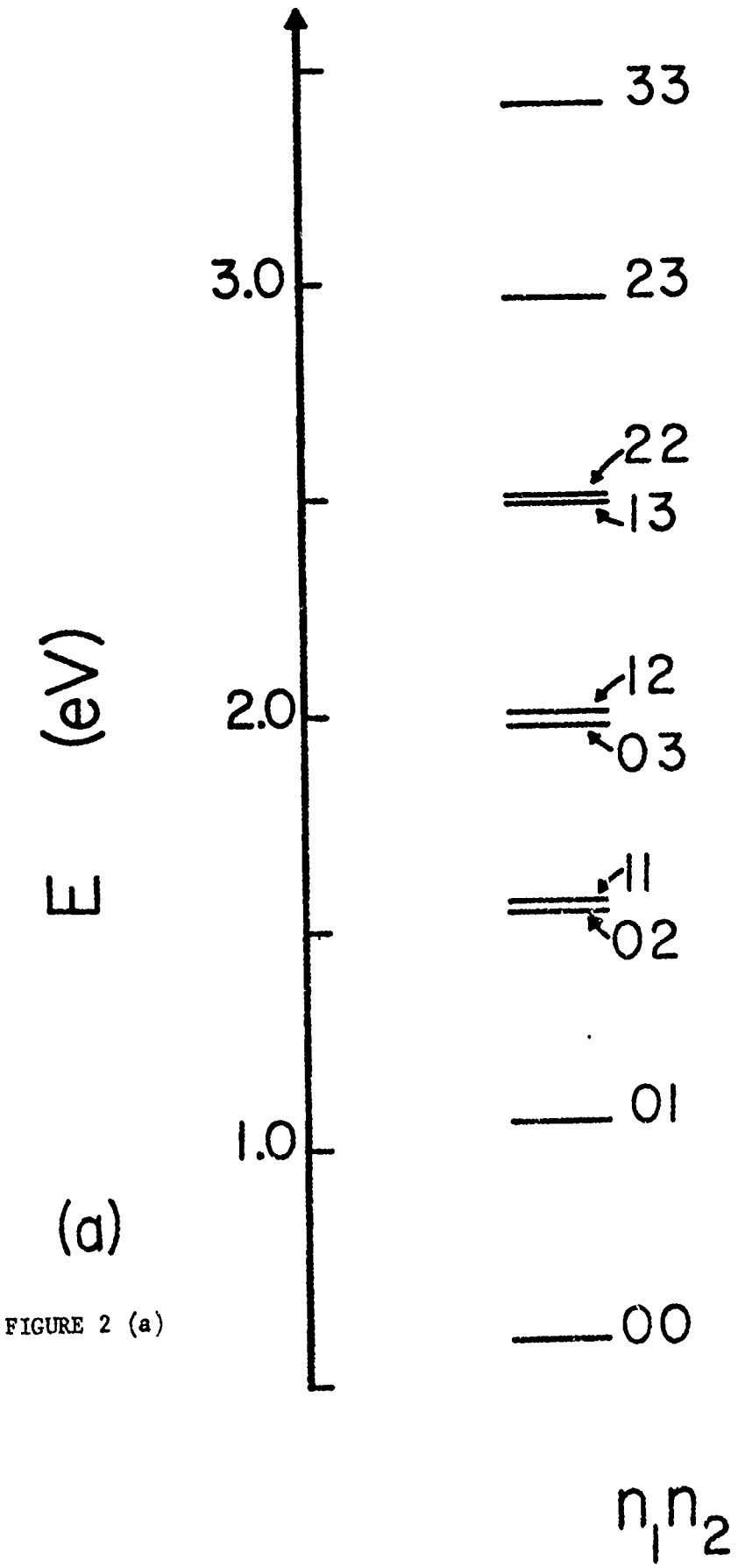

FIGURE 2 (a)

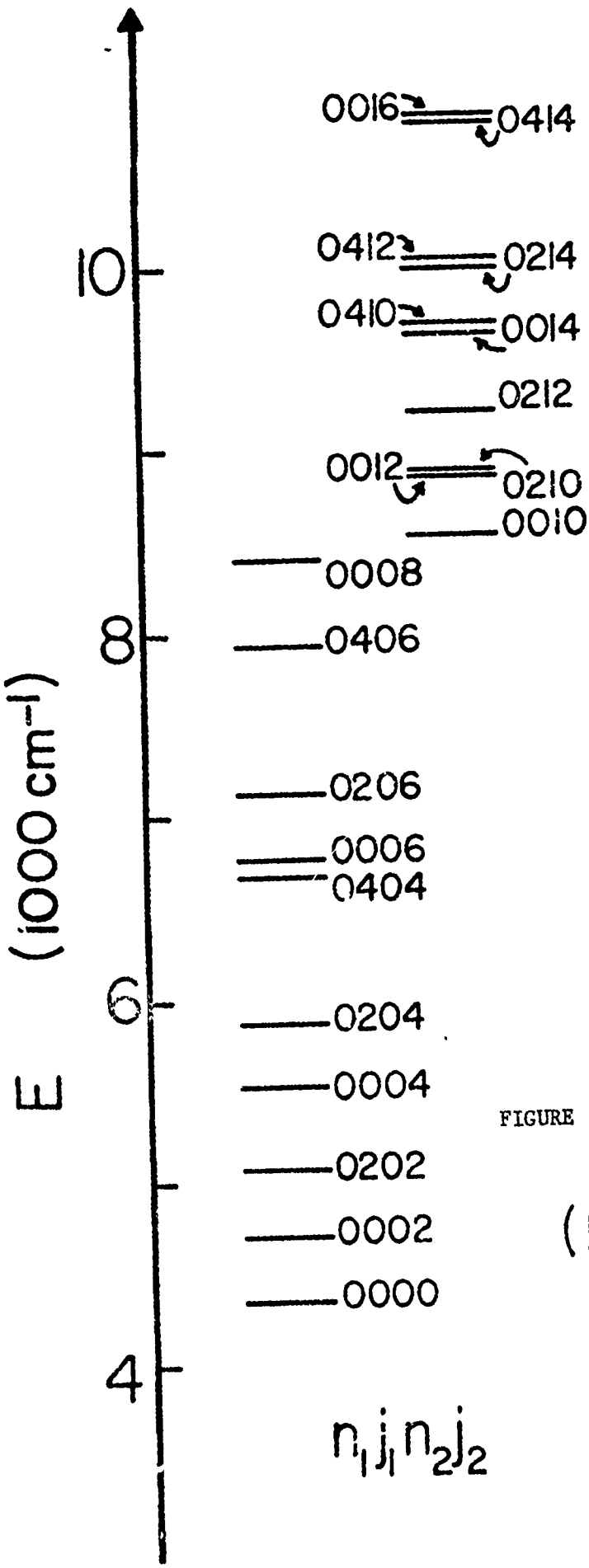
0016
0414
0412
0214
0410
0014
0212
0012
0210
0010
0008
0406
0206
0006
0404
0204
0004
0202
0002
0000
10
8
6
4
E (1000 cm⁻¹)
$n_1 j_1 n_2 j_2$

FIGURE 2 (b)

(b)

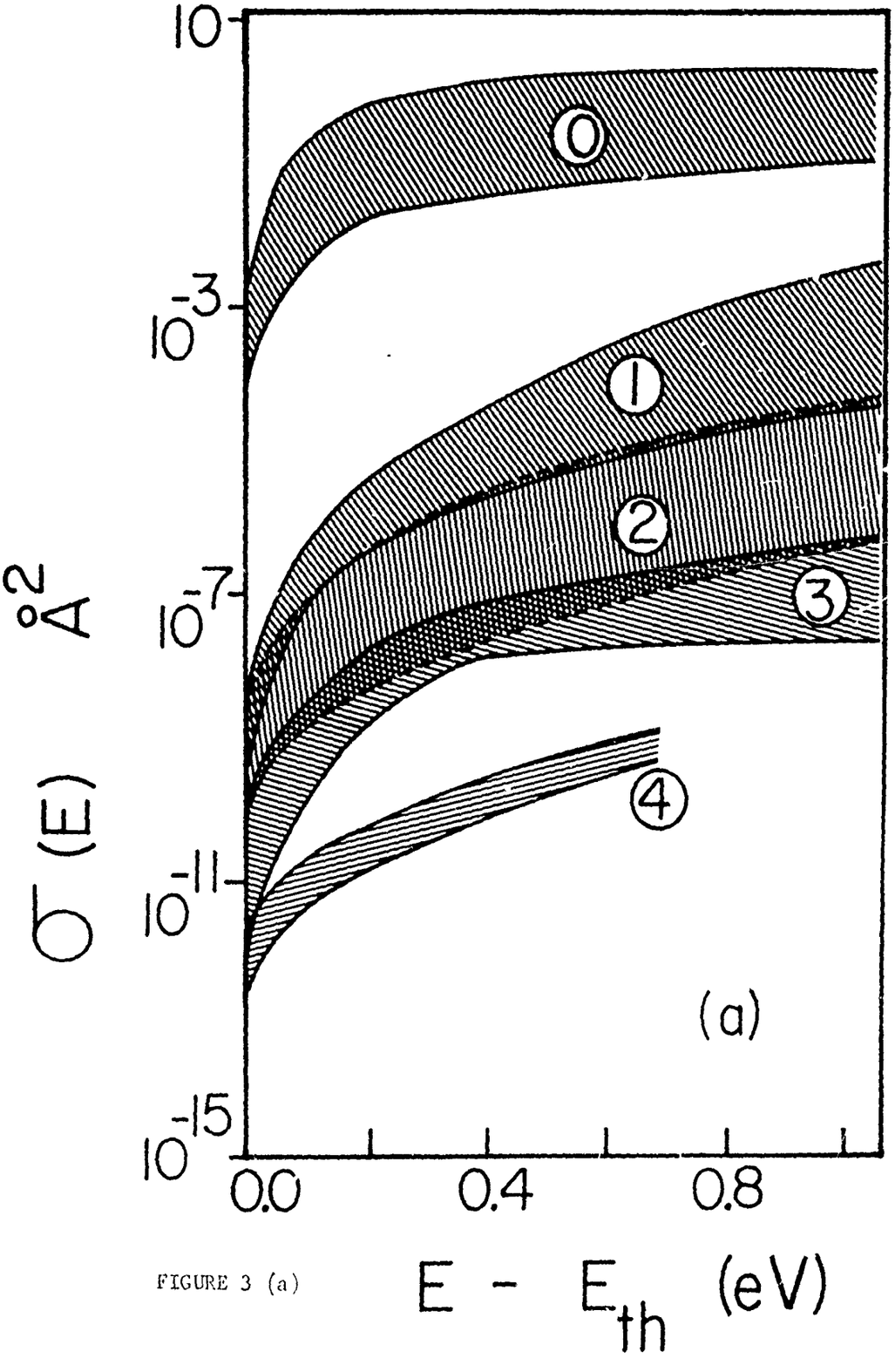

FIGURE 3 (a)

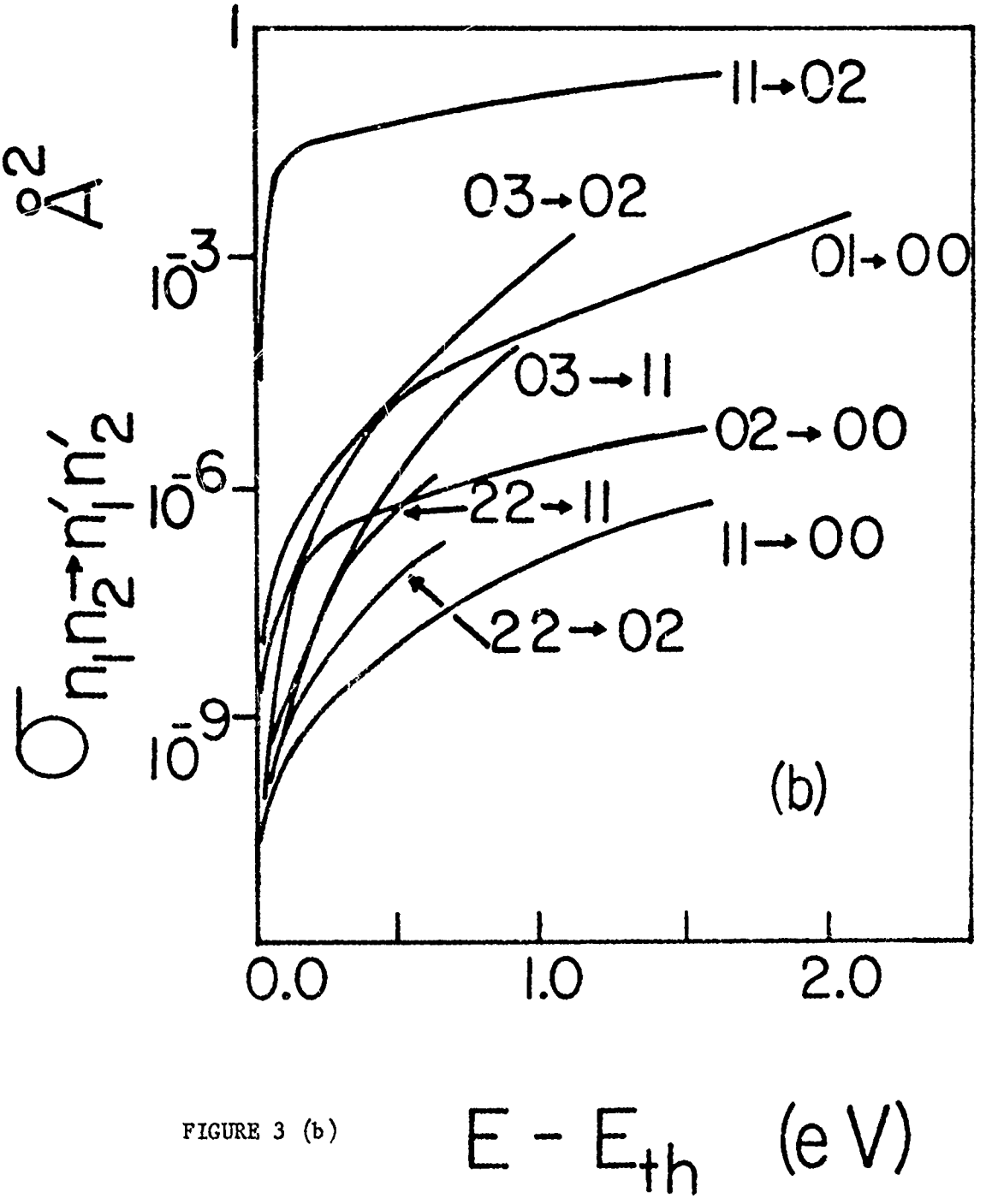
1
10^{-3}
10^{-6}
10^{-9}
$\sigma_{n_1 n_2 \to n_1' n_2'}$ A_o^2
11→02
03→02
01→00
03→11
02→00
22→11
11→00
22→02
(b)
0.0
1.0
2.0
E - E_{th} (eV)

FIGURE 3 (b)

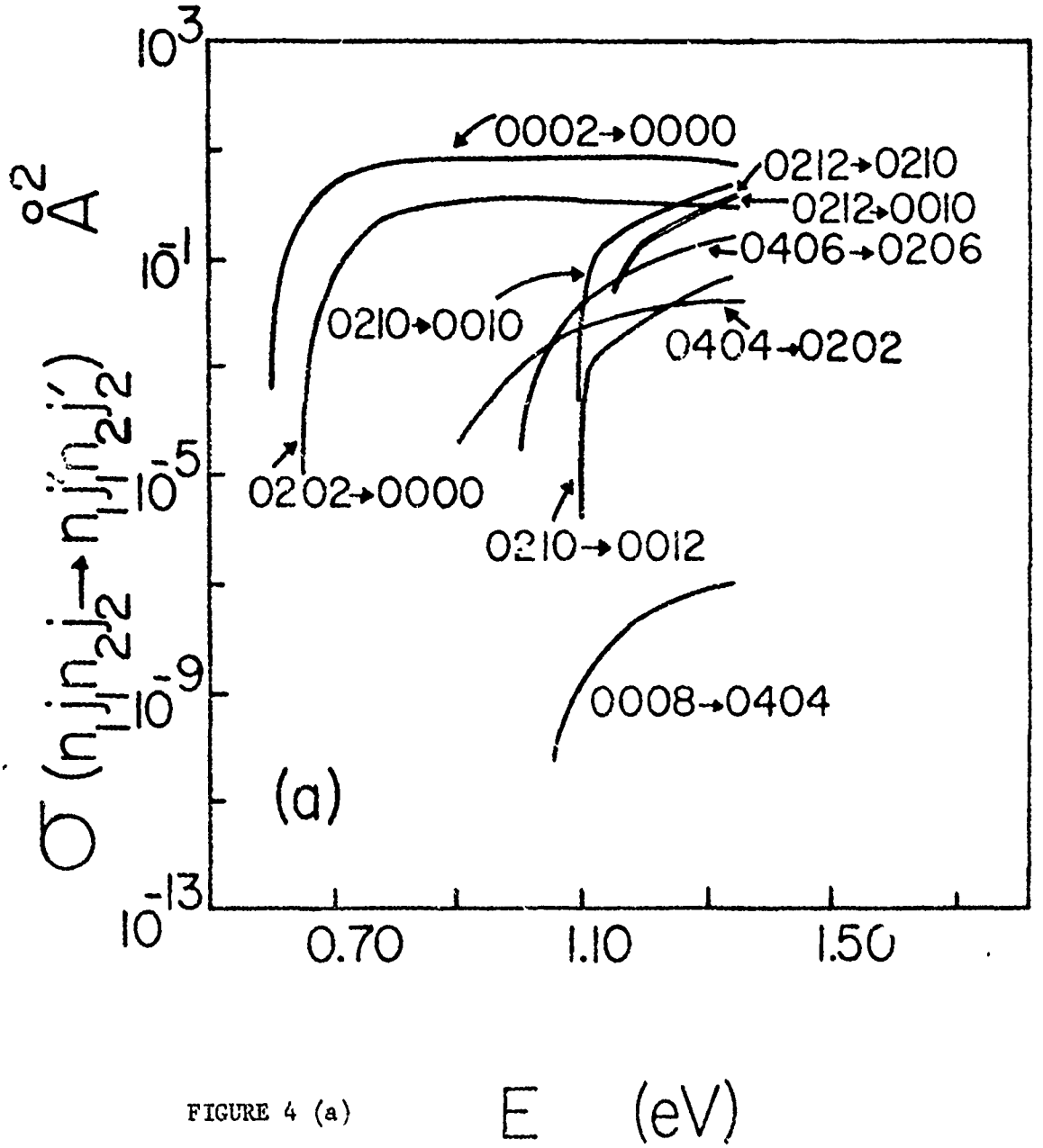
10^3
10^1
10^{-5}
10^{-9}
10^{-13}
$\sigma(n_1 j n_2 j_2 \rightarrow n_1' j' n_2 j_2)$ Å^2
0002→0000
0212→0210
0212→0010
0406→0206
0210→0010
0404→0202
0202→0000
0210→0012
0008→0404
(a)
0.70
1.10
1.50
E (eV)

FIGURE 4 (a)

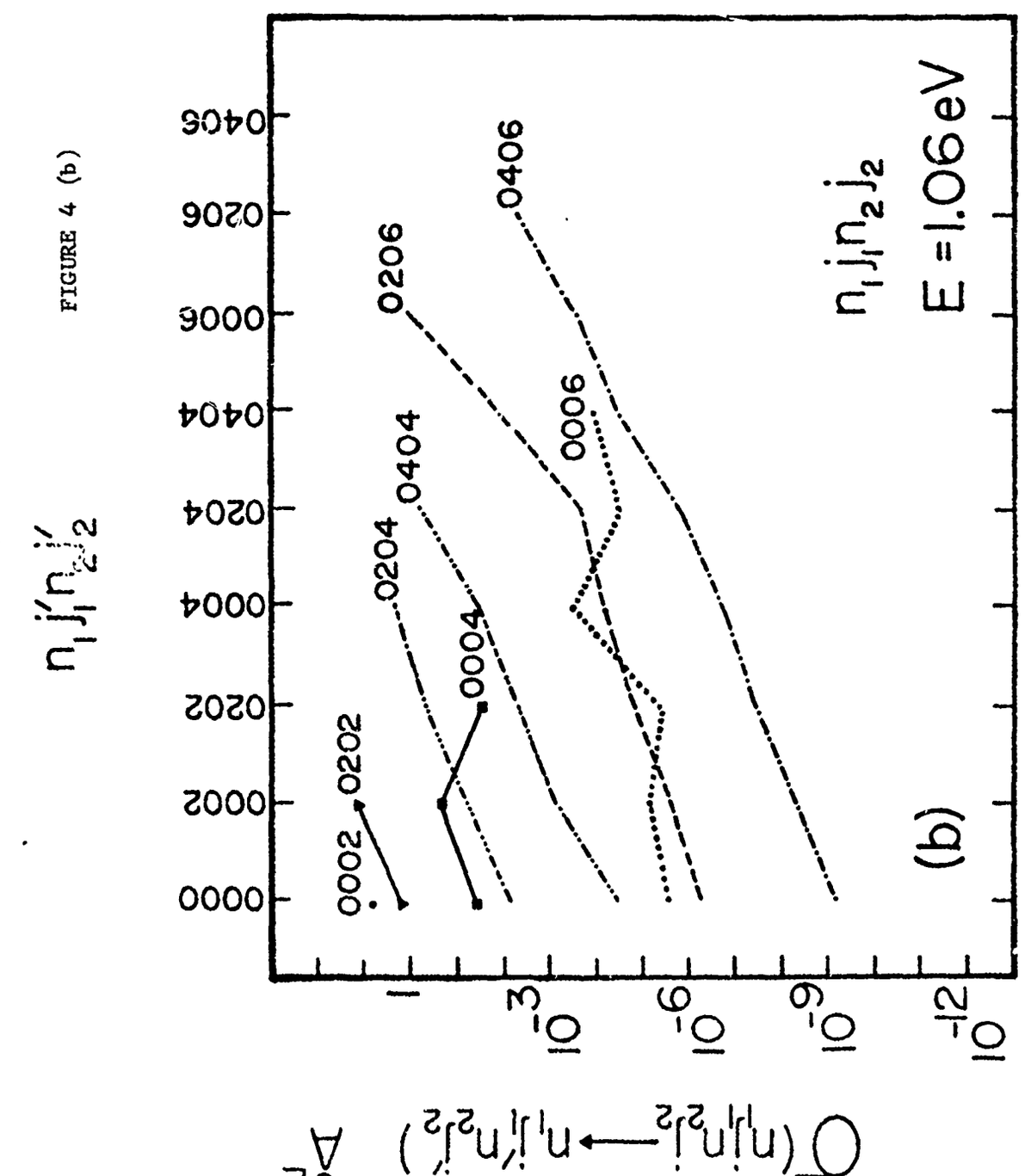
$\sigma(n_1 j_1 n_2 j_2 \rightarrow n_1 j_1' n_2 j_2')$ $A^{\circ 2}$
10^{-12}
10^{-9}
10^{-6}
10^{-3}
1
0000
0002
0202
0004
0204
0404
0006
0206
0406
$n_1 j_1 n_2 j_2$
E = 1.06 eV
(b)
$n_1 j_1' n_2 j_2'$

FIGURE 4 (b)

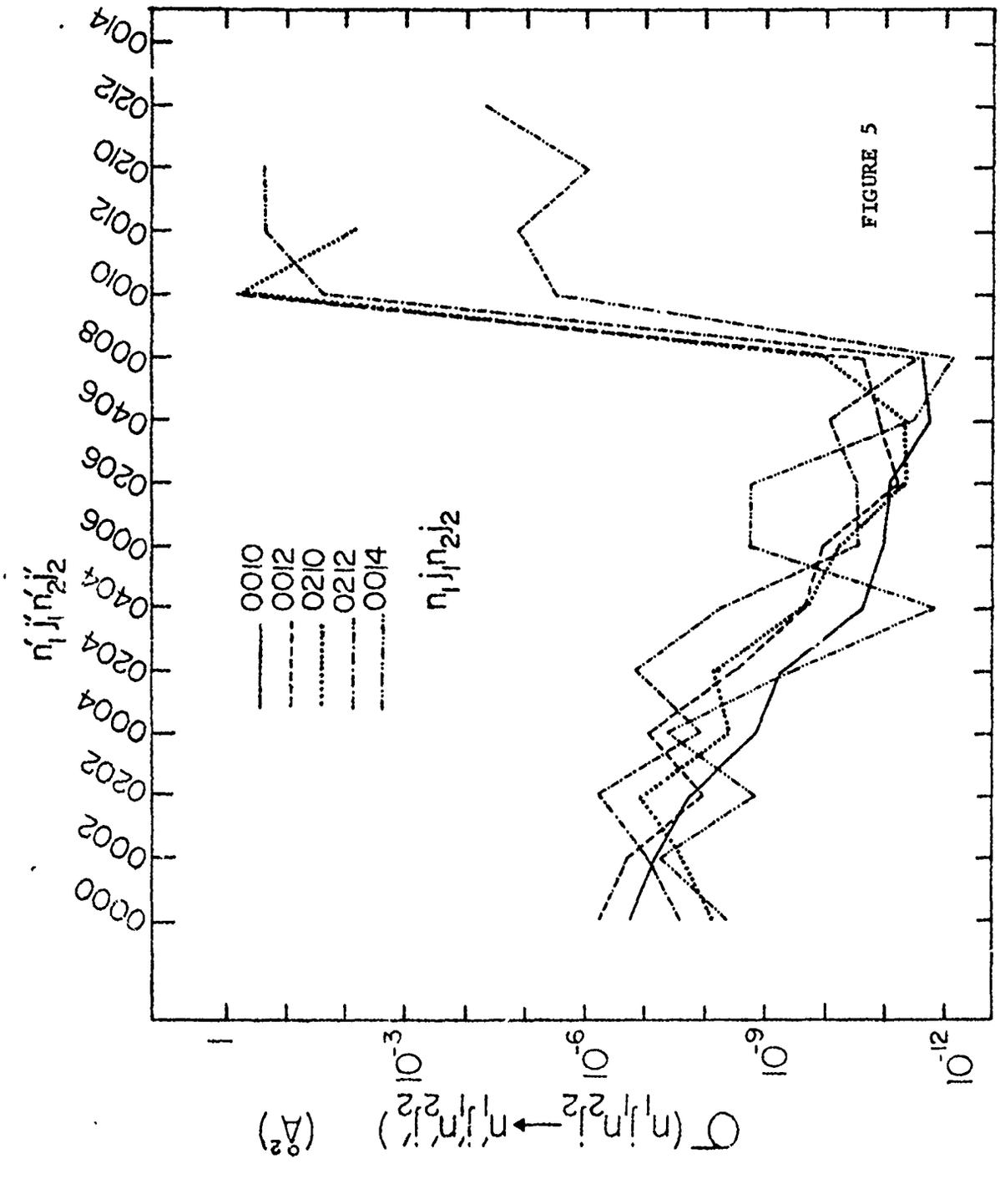
$\sigma(n_1 j_1 n_2 j_2 \rightarrow n_1' j_1' n_2' j_2')$ (Å²)
10^{-3}
10^{-6}
10^{-9}
10^{-12}
1
$n_1' j_1' n_2' j_2'$
0000
0002
0202
0004
0204
0404
0006
0206
0406
0008
0010
0012
0210
0212
0014
$n_1 j_1 n_2 j_2$
0010
0012
0210
0212
0014

FIGURE 5

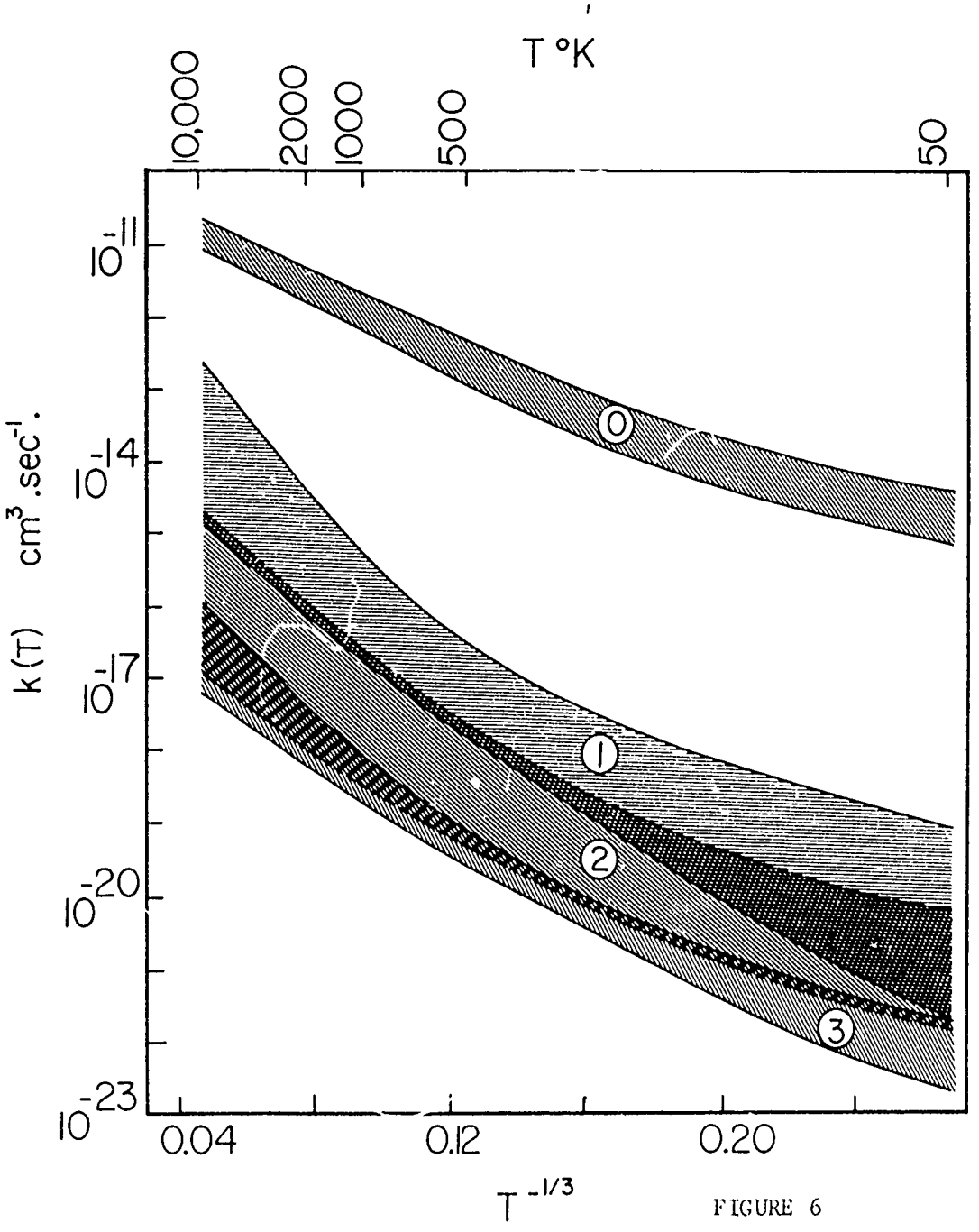
T °K
10,000
2000
1000
500
50
10^{-11}
10^{-14}
10^{-17}
10^{-20}
10^{-23}
k(T) cm³.sec⁻¹.
0
1
2
3
0.04
0.12
0.20
T -1/3

FIGURE 6

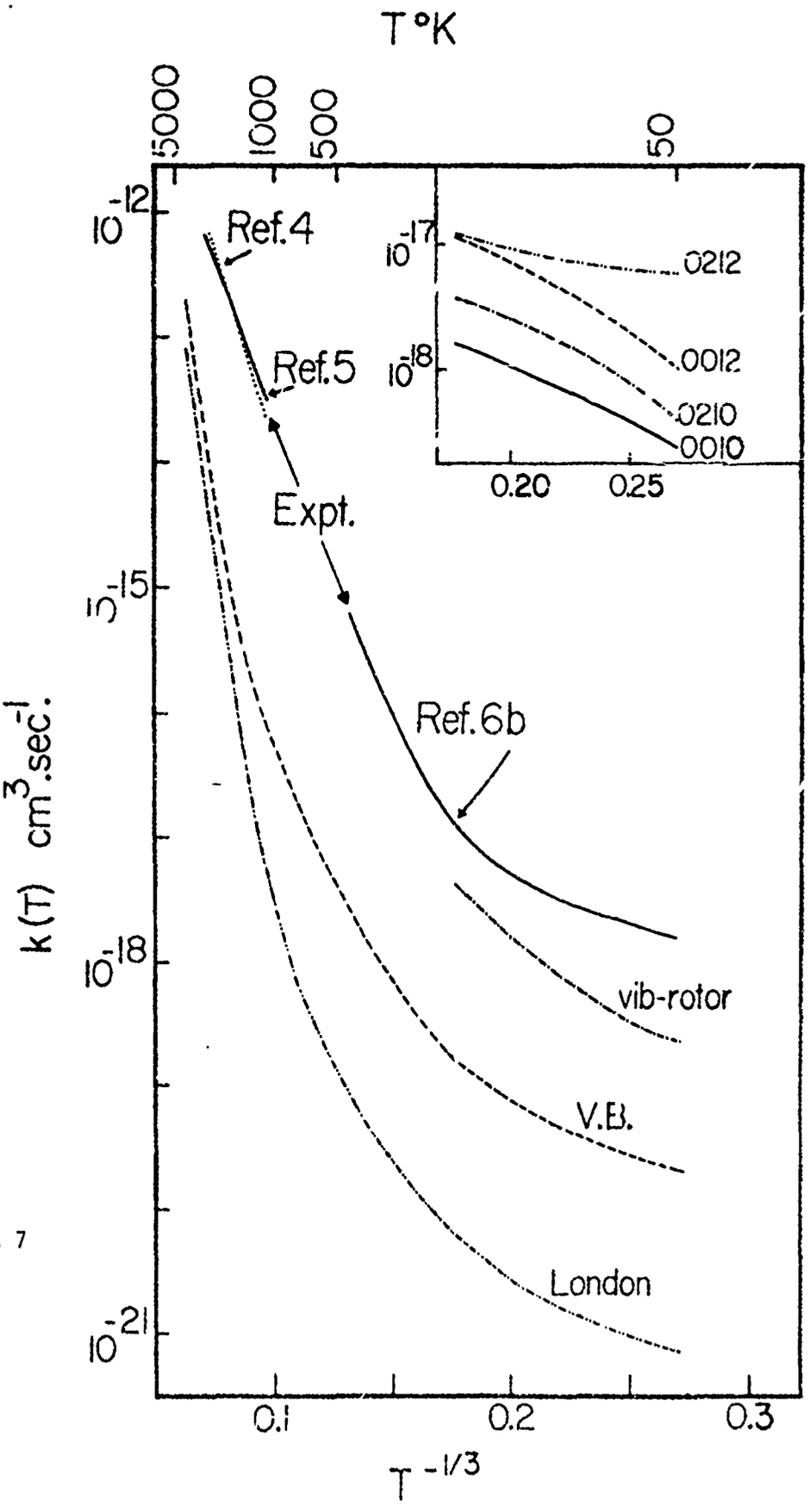
T °K
5000
1000
500
50
Ref.4
Ref.5
Expt.
Ref.6b
vib-rotor
V.B.
London
0212
0012
0210
0010
0.20
0.25
k(T) cm³.sec⁻¹
T⁻¹/³
0.1
0.2
0.3

FIGURE 7

STOCHASTIC THEORY OF MOLECULAR COLLISIONS II: APPLICATION TO ATOM-VIBROTOR COLLISIONS.

by

Stuart D. Augustin

and

Herschel Rabitz*

Department of Chemistry

Princeton University

Princeton, New Jersey 08540

ABSTRACT

In this work stochastic theory is applied to the treatment of atom-vibrotor collisions. This is an extension of a previous paper which described molecular collisions by a Pauli master equation or a Fokker-Planck equation. In this framework an energy conserving classical path model is explored, and methods for solving the equations numerically are discussed. The coefficients of the Fokker-Planck equation are shown to be expressible as simple functions of the interaction potential. Estimates of the computational labor are also discussed. Finally as a follow-up on the initial work, numerical solutions of the master equation for the collinear vibrational excitation problem of Secrest and Johnson are presented in an Appendix.

I. INTRODUCTION

Many important and interesting gas phase phenomena involve collisions of relatively large and complex particles. A previous paper[1] (hereafter referred to as I) investigated treating molecular collisions as a process of probability diffusion between quantum states. This avenue of approach seems attractive for handling complex collision systems that are too difficult to treat by standard methods. These ideas are more fully developed in the present paper.

The treatment in I presented equations that are applicable, in principle, to arbitrary systems. However, the theory was only developed in detail for one-dimensional problems (i.e., one internal degree of freedom). The present paper concentrates on an atom-vibrotor collision system as the simplest meaningful case with more than one degree of freedom. The resulting stochastic equations then have two spatial variables, one for vibration and one for rotation. All the relevant concepts can then be generalized in a straightforward fashion to arbitrary inelastic scattering problems.

The stochastic theory requires the solution of either a master equation (ME) or a simpler Fokker-Planck equation (FPE). One of the most desirable aspects of this theory is that all the physics of the collision system can be condensed into a small number of coefficient functions in a FPE. Qualitative predictions about the behavior of the inelastic processes can then be immediately made by considering the magnitude and form of these functions. It will be shown in this work how the FPE coefficients can be generated in a straightforward fashion from a given intermolecular potential. This approach may ultimately prove to be useful for relating observed cross sections to the properties of an individual collision system (i.e., the Hamiltonian).

In most cases of practical interest, the ME or FPE will not be analytically solvable. This paper therefore explores methods of solving these equations numerically. The translational degree of freedom (represented by the vector $\vec{R}$) is treated in this context as following an energy conserving classical trajectory. For most problems of chemical interest the particles are massive enough so that the classical path approximation is expected to be very good. The combination of a classical translational path with internal degrees of freedom obeying quantum stochastic equations of motion provides an attractive conceptual model for molecular collisions.

Section II deals with the detailed consideration of the stochastic theory as applied to atom-vibrotor scattering. It is shown that the ME can be approximated by a FPE which describes the flow of probability between energy levels rather than quantum numbers. This has important advantages, especially for cases such as asymmetric rotors where the quantum numbers are poorly defined. Expressions for the FPE coefficients are developed in terms of matrix elements of simple functions of the interaction potential. Applications of various approximate methods to the stochastic equations are considered in Section III.

Numerical methods of solution are treated in Section IV. Given an interaction potential, an energy conserving classical path model for the ME requires that an exponential matrix be calculated at each step of the R integration. If n is the total number of quantum states, this procedure will typically require matrix multiplications whose computational difficulty varies as n^3. The FPE, on the other hand, can be solved in principle by methods whose difficulty is more dependent on the number of degrees of freedom, N, than the number of states. The relative computational efforts can be of considerable practical importance.

Finally, calculations were presented in I for a collinear vibrational excitation problem. It is shown in this paper that some of the approximations involved in those calculations can be eliminated or improved. In particular the classical path formulation of Section II is illustrated. Results for the model He-H_2 collinear system of Secrest and Johnson are presented in an Appendix. In addition it is shown in Section II that the stochastic equations remain very easy to solve, even for noncollinear collisions, whenever the intermolecular potential has the form

$$V = A(\vec{R}) + B(\vec{R})\,C(\vec{r})$$

where $\vec{r}$ is shorthand for all the internal degrees of freedom. The present paper further develops the ideas presented in I, but much additional work is still to be performed.

II. STOCHASTIC THEORY OF ATOM-VIBROTOR COLLISIONS

It was shown in I that the ME for a collision system with N internal degrees of freedom is given by

$$\frac{\partial}{\partial t}P\left(x_1,x_2,\ldots,x_N,t\right) = \sum_{x_1',x_2',\ldots x_N'} A\left(x_1',\ldots,x_N';x_1,\ldots,x_N;t\right)\ P\left(x_1',x_2',\ldots,x_N',t\right) \qquad (2.1$$

where x_i is a (discrete) index for the i-th degree of freedom. If the microscopic transition rates A are strongly peaked about $x_i = x_i'$, then $P\left(x_1',x_2',\ldots,x_N',t\right)$ can be expanded in an N dimensional Taylor series about the diagonal values. The FPE is obtained by retaining in this expansion only terms through second order. It will therefore contain N terms of the form $\frac{\partial P}{\partial x_i}$, N terms of the form $\frac{\partial^2 P}{\partial x_i^2}$, and $(N-1)$ terms of the form $\frac{\partial^2 P}{\partial x_i \partial x_j}$. Since the mixed partial derivative cross terms only occur pairwise, all the essential features are contained in a two-dimensional example. In the remainder of this paper we shall use an atom-vibrotor as a prototype two-dimensional problem.

A. The ME for an Atom-Vibrotor System

The relevant ME is

$$\frac{\partial}{\partial t}P^J(n,j,t) = \sum_{n',j'} A^J(n,j;n',j';t)\ P^J(n',j',t) \qquad (2.2)$$

where n is the vibrational quantum number, j is the rotational quantum number, and J is the total angular momentum. The microscopic transition rates in Eq.(2.2) are given by (see I)

$$\tau A^J(n,j;n',j';t) = \left|\langle n,j|\exp(-iV\tau/\hbar)|n',j'\rangle\right|^2 - \delta_{nn'}\delta_{jj'} \qquad (2.3)$$

where V is the intermolecular potential and τ is the (generally time-dependent) increment between time steps. Normally the orbital angular momentum ℓ should be included in Eq.(2.3), but it is assumed to be eliminated by using an effective Hamiltonian.[2] Note that V is a function of the translational coordinate $\vec{R}$ so that Eqs.(2.2) and (2.3) assume that $\vec{R}$ is a known function of time.

It was shown in I that the above ME involves approximations whose validity depends on the size of τ. Most important of these is the use of the repeated randomness assumption in the strong interaction region of the collision. This requires that the probability amplitudes accumulate enough phase in the time interval t to $t+\tau$ for the random phase approximation to be made <u>at each step</u>. If τ is too small, the phase accumulation will not be large enough and the ME will not be a good approximation. This restriction does not apply to the weak interaction region where only a small fraction of the inelasticity is presumed to occur.

There are also constraints on the largest permissible value of τ. The time interval τ should, clearly, be short compared to the duration of the collision. It may also be noted that the time derivative in Eq.(2.2) was obtained as a small τ approximation to the finite difference expression

$$\frac{\partial}{\partial t}P^J(n,j,t) \approx \frac{P^J(n,j,t+\tau) - P^J(n,j,t)}{\tau} \qquad (2.4)$$

The above arguments indicate that τ has an optimum value determined by the characteristics of the system at each point in time. It was suggested in I that the average value of the time required for a jump between adjacent quantum states was a good estimate for τ. This should also be reasonably close to the shortest time interval for which the difference equations are numerically stable. If H_0 is the Hamiltonian for the internal modes (n and j) and ϵ_{nj} are its eigenvalues, the prescription for $\tau(t)$ becomes

$$\tau(t) = \sum_{n,j} P(n,j,t) \frac{\Delta\epsilon_{nj}}{\sqrt{\left\langle \left| \frac{dH_0}{dt} \right|^2 \right\rangle_{nj}}}$$

$$= \hbar \sum_{n,j} P(n,j,t) \frac{\Delta\epsilon_{nj}}{\left\{ \sum_{n',j'} \left(\epsilon_{nj} - \epsilon_{n'j'}\right)^2 \left| V_{nj,n'j'} \right|^2 \right\}^{1/2}} \qquad (2.5)$$

In Eq.(2.5), $\Delta\epsilon_{nj}$ should be interpreted as the mean of the energy gaps between nj and the adjacent quantum states. The best form for this is not entirely clear at present although there is no difficulty for a pure vibrational problem or a pure rotational problem. In these cases the geometric mean of the two nearest energy differences is indicated. For a harmonic oscillator $\Delta\epsilon_n$ just reduces to the constant energy spacing $\hbar\omega$. The stability criterion of Eq.(4.11) may provide a suitable alternative prescription for τ in the atom-vibrotor case. Practical calculations would also be very helpful in this regard.

The ME is still not complete until $\vec{R}(t)$ is known. One way of specifying this is to assume that the translational degree of freedom follows a classical trajectory. If the coupling between translation and internal

modes is then ignored, simple models can be developed for the inelastic scattering.[1] A simplified form of Eq.(2.5) such as

$$\tau(t) = \hbar \Delta\epsilon_{n_0 j_0} \left[\sum_{n',j'} \left(\epsilon_{n_0 j_0} - \epsilon_{n'j'}\right)^2 \left|V_{n_0 j_0, n'j'}\right|^2 \right]^{-1/2} \qquad (2.6)$$

(n_0, j_0 is the initial state) would be appropriate in this case. It should be noted that when τ is an appreciable fraction of the collision time, the time derivative in Eq.(2.2) should properly be written as a finite difference (see Eq.(2.4)). In this case calculations which treat (2.2) as a differential equation in time may significantly overestimate the interaction as a result. However, both the translational decoupling and small τ approximations are quite good in the limit of a large number of strongly coupled internal states.

Given the prescription in Eq.(2.6), the ME is very easy to solve if V_r is time independent. It is easy to see that this will be true whenever the potential has the general form

$$V = A(\vec{R}) + B(\vec{R})\, C(\vec{r}) \qquad (2.7)$$

where $\vec{r}$ indicates the relative separation vector of the diatom. Inserting Eq.(2.7) into Eq.(2.6) gives

$$\tau(t) = \hbar \Delta\epsilon_{n_0 j_0} \left[\sum_{n',j'} \left(\epsilon_{n_0 j_0} - \epsilon_{n'j'}\right)^2 \left|C_{n_0 j_0, n'j'}\right|^2 \right]^{-1/2} / B(\vec{R}) \qquad (2.8)$$

Thus the rates in Eq.(2.3) become

$$\tau(t)\, A^{J}(n,j;n',j';t) =$$

$$\left| \langle n,j | \exp \left[\frac{-\, i\, \Delta\epsilon_{n_0 j_0}\, C(\vec{r})}{\sum_{n'',j''} \left(\epsilon_{n_0 j_0} - \epsilon_{n'' j''} \right)^2 \left| C_{n_0 j_0, n'' j''} \right|^2} \right] | n',j' \rangle \right|^2 - \delta_{nn'}\, \delta_{jj'} \qquad (2.9$$

All of the time dependence in the rate matrix $\underset{\sim}{A}$ is now seen to be contained in the multiplicative factor $1/\tau(t)$ so that the solution of Eq.(2.2) is the exponential of a time independent matrix multiplied by a function of time.

These simple models have the disadvantage that the classical trajectory, $\vec{R}(t)$, is not coupled to the internal degrees of freedom. Since this will not conserve the total energy, the results can be unsatisfactory when the energy transfer in the collision is an appreciable fraction of the translational energy. One way of remedying this problem is to force conservation of energy by defining the instantaneous radial velocity as[3]

$$\frac{dR}{dt} = \pm \left\{ 2/\mu \left[E - \langle \ell^2 \rangle / 2\mu R^2 - \langle H_0 \rangle - \langle V \rangle \right] \right\}^{1/2} \qquad (2.10)$$

Practical application of this approach will, of course, require that $R(t)$ be computed numerically from Eq.(2.10) while the internal modes are propagated by Eq.(2.2). The sign of $\frac{dR}{dt}$ is not determined by Eq.(2.10) so that it may be advantageous to integrate the momentum conjugate to R as well (see Section IV). Expectation values of H_0 and V are conveniently given by

$$\langle H_0 \rangle = \sum_{n,j} \epsilon_{nj} P(n,j,t) \tag{2.11a}$$

$$\langle V \rangle = \sum_{n,j} \sum_{n',j'} \sqrt{P(n,j,t)\, P(n',j',t)}\ \langle n,j|V(R)|n',j'\rangle \tag{2.11b}$$

although other choices are possible. The orbital angular momentum ℓ may be treated as a constant within an effective Hamiltonian formulation,[2] or $\langle \ell^2 \rangle$ can be expressed in a proper coupled angular momentum representation.

B. The FPE for an Atom-Vibrotor System

For this special case the FPE is obtained by a Taylor expansion of $P(n',j',t)$ in Eq.(2.2). However, this expansion could either be in terms of the quantum numbers n,j or the corresponding energy states ϵ_n, ϵ_j. It can be shown that these two approaches are equivalent in that their finite difference approximations both match the ME through second order (see Section IV). However, it will be shown below that if the expansion is performed in terms of the energy levels, the FPE coefficients are expressible as matrix elements of simple functions of the interaction potential. This is in contrast to the development in I, which utilized expansions in the quantum numbers. The two methods are identical whenever the energy levels are evenly spaced as for a harmonic oscillator.

The FPE in energy variables is now

$$\frac{\partial}{\partial t}P^J\left(\epsilon_n,\epsilon_j,t\right) = B_1 \frac{\partial}{\partial \epsilon_n}P^J\left(\epsilon_n,\epsilon_j,t\right) + B_2 \frac{\partial^2}{\partial \epsilon_n^2}P^J\left(\epsilon_n,\epsilon_j,t\right)$$

$$+ C_1 \frac{\partial}{\partial \epsilon_j}P^J\left(\epsilon_n,\epsilon_j,t\right) + C_2 \frac{\partial^2}{\partial \epsilon_j^2}P^J\left(\epsilon_n,\epsilon_j,t\right) + D \frac{\partial^2}{\partial \epsilon_n \partial \epsilon_j}P^J\left(\epsilon_n,\epsilon_j,t\right) \quad (2.12)$$

where the coefficients are given by

$$B_k = \frac{1}{k!} \sum_{n',j'} \left(\epsilon_{n'} - \epsilon_n\right)^k A^J\left(n,j;n',j';t\right) \quad (2.13a)$$

$$C_k = \frac{1}{k!} \sum_{n',j'} \left(\epsilon_{j'} - \epsilon_j\right)^k A^J\left(n,j;n',j';t\right) \quad (2.13b)$$

$$D = \sum_{n',j'} \left(\epsilon_{n'} - \epsilon_n\right)\left(\epsilon_{j'} - \epsilon_j\right) A^J\left(n,j;n',j';t\right) \quad (2.13c)$$

The sums in Eqs.(2.13a,b,c) can be performed analytically. First define m to be the reduced mass of the diatom and $u = (r - r_e)$ to be the vibrational displacement. The internal Hamiltonian H_0 can be decomposed as

$$H_0 = H_v + H_r$$

where

$$H_v = p_u^2/2m + V_0(u) \quad (2.14a)$$

$$H_r = \hat{j}^2/2mr^2 \quad (2.14b)$$

and

$$H_v|n,j\rangle = \epsilon_n|n,j\rangle \tag{2.15a}$$

$$H_r|n,j\rangle = \epsilon_j|n,j\rangle \tag{2.15b}$$

These last two equations assume that rotation and vibration are separable, but this approximation can be easily removed. The various ϵ's in Eqs.(2.13a,b,c) can now be replaced by H_v and H_r. Inserting Eq.(2.3) into the expression for B_1, Eq.(2.13a), yields

$$\tau B_1 = \sum_{n',j'} \langle n,j|\exp(iV\tau/\hbar)|n',j'\rangle\langle n',j'|(H_v - \epsilon_n)\exp(-iV\tau/\hbar)|n,j\rangle \tag{2.16}$$

Noting that $\sum_{n',j'} |n',j'\rangle\langle n',j'|$ is just the unit operator leads to the result

$$\tau B_1 = \langle n,j|\exp(iV\tau/\hbar)(H_v - \epsilon_n)\exp(-iV\tau/\hbar)|n,j\rangle \tag{2.17}$$

It is convenient to define new states $|\psi_v\rangle$ and $|\psi_r\rangle$ by

$$|\psi_v\rangle = \exp(iV\tau/\hbar)(H_v - \epsilon_n)\exp(-iV\tau/\hbar)|n,j\rangle \tag{2.18a}$$

$$|\psi_r\rangle = \exp(iV\tau/\hbar)(H_r - \epsilon_j)\exp(-iV\tau/\hbar)|n,j\rangle \tag{2.18b}$$

This allows Eqs.(2.13a,b,c) to be compactly written as

$$\tau B_1 = \langle n,j|\psi_v\rangle \tag{2.19a}$$

$$2\tau B_2 = \langle \psi_v|\psi_v\rangle \tag{2.19b}$$

$$\tau C_1 = \langle n,j|\psi_r\rangle \tag{2.19c}$$

$$2\tau C_2 = \langle \psi_r|\psi_r\rangle \tag{2.19d}$$

$$\tau D = \langle \psi_r|\psi_v\rangle \tag{2.19e}$$

Furthermore Eq.(2.18a) can be rewritten as

$$|\psi_v\rangle = \exp(iV\tau/\hbar)\left[(H_v - \epsilon_n),\ \exp(-iV\tau/\hbar)\right]|n,j\rangle$$

where $[\cdot,\cdot]$ is the commutator bracket. Therefore, it is easy to see that

$$|\psi_v\rangle = \frac{1}{2m}\left\{i\tau\hbar\frac{\partial^2 V}{\partial u^2} + \tau^2\left(\frac{\partial V}{\partial u}\right)^2 - 2\tau\left(\frac{\partial V}{\partial u}\right)p_u\right\}|n,j\rangle \tag{2.20a}$$

and in a similar fashion

$$2mr^2|\psi_r\rangle = \left\{\tau^2(1-x^2)\left(\frac{\partial V}{\partial x}\right)^2 + \frac{i\tau}{\hbar}\left[\frac{\partial}{\partial x}(1-x^2)\frac{\partial V}{\partial x}\right] + \frac{2i\tau}{\hbar}\frac{\partial V}{\partial x}G\right.$$

$$\left. - \frac{2\tau}{(1-x^2)}\frac{\partial V}{\partial \varphi}J_z + \frac{\tau^2}{(1-x^2)}\left(\frac{\partial V}{\partial \varphi}\right)^2 + \frac{i\tau\hbar}{(1-x^2)}\frac{\partial^2 V}{\partial \varphi^2}\right\}|n,j\rangle \tag{2.20b}$$

where [4] $x = \cos\theta$ and the operator G is defined by[5]

$$G|j\rangle = \frac{j(j+1)}{\sqrt{2j+1}} \left\{ \frac{|j-1\rangle}{\sqrt{2j-1}} - \frac{|j+1\rangle}{\sqrt{2j+3}} \right\}$$

The three φ dependent terms in Eq.(2.20b) can be removed by transforming to the body-fixed (BF) reference frame[6] or by using an effective Hamiltonian approximation.[2]

The new states $|\psi_v\rangle$, $|\psi_r\rangle$ have an interesting physical interpretation. From the Heisenberg equations of motion

$$\dot{H}_v = \frac{dH_v}{dt} = -\frac{1}{2m}\left(\frac{\partial V}{\partial u}p_u + p_u\frac{\partial V}{\partial u}\right)$$

$$= \frac{1}{2m}\left(i\hbar\frac{\partial^2 V}{\partial u^2} - 2\frac{\partial V}{\partial u}p_u\right) \qquad (2.21a)$$

and

$$\dot{H}_r = \frac{i\tau}{\hbar}\left[\frac{\partial}{\partial x}(1-x^2)\frac{\partial V}{\partial x}\right] + 2i\tau\hbar\frac{\partial V}{\partial x}G + \frac{i\tau\hbar}{(1-x^2)}\frac{\partial^2 V}{\partial\varphi^2} - \frac{2\tau}{(1-x^2)}\frac{\partial V}{\partial\varphi}J_z \qquad (2.21b)$$

The states $|\psi_r\rangle$, $|\psi_v\rangle$ can, therefore, be expressed in the form

$$|\psi_v\rangle = \left[\tau\dot{H}_v + \frac{\tau^2}{2m}\left(\frac{\partial V}{\partial u}\right)^2\right]|n,j\rangle \qquad (2.22$$

$$2mr^2|\psi_r\rangle = \left[\tau\dot{H}_r + \frac{\tau^2}{(1-x^2)}\left(\frac{\partial V}{\partial\varphi}\right)^2 + \tau^2(1-x^2)\left(\frac{\partial V}{\partial x}\right)^2\right]|n,j\rangle \qquad (2.22$$

which are of the form of τ times a rate of energy transfer plus τ^2 times a dispersive term.

III. APPROXIMATION METHODS AND THE STOCHASTIC THEORY

Various standard approximation schemes for inelastic scattering can be incorporated in the stochastic theory. In this regard it has been shown above that the FPE coefficients can be obtained directly from the potential. The properties of these coefficients, without further computation, may then be used as a simple guide to the behavior of the collision system or may provide physical insight into the approximation methods. For example, in this section we shall consider the combination of breathing sphere and effective Hamiltonian methods with the stochastic theory.

Effective Hamiltonian methods reduce the dimensionality of a close coupled calculation by preaveraging or eliminating angular momentum projections before doing the collision dynamics.[2] The centrifugal decoupling (CD) approximation[7] is easily incorporated into a formulation of the ME or FPE. Use of an effective potential[8] with the FPE is inconvenient unless a V_{eff} operator can be defined, thus permitting the use of Eqs.(2.20a,b). However, it has recently been shown that modified effective potential operators can be defined which retain the same dimensionality reduction as the original formulation.[9]

In the BF reference frame the potential has no dependence on azimuthal angles. Eq.(2.20b) therefore simplifies to

$$2mr^2|\psi_r\rangle = \left\{\tau^2(1-x^2)\left(\frac{\partial V}{\partial x}\right)^2 + i\tau\hbar\left[\frac{\partial}{\partial x}(1-x^2)\frac{\partial V}{\partial x}\right] + 2i\tau\hbar\frac{\partial V}{\partial x}G\right\}|n,j\rangle \quad (3.1)$$

where x is now the cosine of the angle between $\vec{R}$ and $\vec{r}$. The quantum number ω (the projection of the rotational angular momentum on the BF z axis) should also be included in the ME, Eq.(2.2), in this case. Then $\langle \ell^2 \rangle$

in Eq.(2.10) is given by

$$\langle \ell^2 \rangle \simeq J^2 + \langle j^2 \rangle - 2\langle \omega^2 \rangle \tag{3.2}$$

if the CD approximation is used. In an effective potential formulation, on the other hand, ℓ^2 is treated as a constant throughout the collision.

The breathing sphere approximation assumes that there is no strong vibration-rotation coupling. Defining $\bar{P}(\epsilon_n,t)$ as

$$\bar{P}(\epsilon_n,t) = \sum_j P(\epsilon_n,\epsilon_j,t)$$

it is easily seen that $\bar{P}(\epsilon_n,t)$ will satisfy a breathing sphere FPE if the vibrational and rotational parts of Eq.(2.12) are separable. This will be true, for instance, if $D=0$ and if B_1,B_2 have no rotational dependence. Since the coefficients can be obtained relatively easily, it should be possible to determine if a breathing sphere FPE is a good approximation to Eq.(2.12).

IV. NUMERICAL METHODS FOR SOLVING THE STOCHASTIC EQUATIONS

There will obviously be only a small class of scattering problems for which the ME and FPE are analytically solvable. Numerical methods for solving the equations with appropriate boundary conditions are, therefore, considered in this section. Consistent with the goal of describing the scattering process by a simple equation, we shall assume that an effective potential will be used.[8,9] The translational degree of freedom will also be described by an energy-conserving classical path as outlined in Section II.A.

A. Numerical Methods for the ME

Within the classical path approximation, the system is started in an initial state $n_0 j_0$ at a value of R outside the range of the potential. For each value of the orbital angular momentum ℓ, the equations for the internal modes and $R(t)$ are integrated until the particles are separating and R is again outside the range of the potential. Each such "trajectory" will yield the complete vector of transition probabilities into all the possible final states $n_1 j_1$

$$P^{\ell}_{n_0 j_0 \to n_1 j_1}(E)$$

Total cross sections for translational energy E_1 are then computed by

$$\sigma_{n_0 j_0 \to n_1 j_1}(E_1) = \frac{\pi \hbar^2}{2\mu E_1 (2 j_0 + 1)} \sum_{\ell} (2\ell + 1)\, P^{\ell}_{n_0 j_0 \to n_1 j_1}(E) \qquad (4\ 1)$$

Internal state probabilities are propagated from time t to $t+\tau$ by the finite difference form of the ME

$$P^{\ell}(n,j,t+\tau) = \sum_{n',j'} \left|\langle n,j|\exp[-iV(R)\tau/\hbar]\,|n',j'\rangle\right|^2 P^{\ell}(n',j',t) \qquad (4.2)$$

where τ is given by Eq.(2.5). The translational degree of freedom is handled by numerically integrating the equations

$$\dot{R} = \text{sign}(p_R) \times \left\{2\left[E - \hbar^2\ell(\ell+1)/2\mu R^2 - \langle H_0\rangle - \langle V\rangle\right]/\mu\right\}^{1/2} \qquad (4.3)$$

$$\dot{p}_R = \mu\ddot{R} = \hbar^2\ell(\ell+1)/\mu R^3 - \frac{\partial}{\partial R}\langle V\rangle \qquad (4.4)$$

with step size τ. Since p_R is only needed to determine the sign of $\dot{R}$, it does not matter that Eq.(4.4) will not conserve energy. At the end of each time step p_R can be set equal to μ times $\dot{R}$ computed from Eq.(4.3). An application of these ideas to a collinear vibrator is presented in the Appendix.

When the dimensionality n of the problem is reasonably large, the major computational expense of this procedure is the evaluation of the microscopic transition rates on the R.H.S. of Eq.(4.2). This would normally involve the numerical exponentiation of a matrix whose elements are

$$-i\tau\langle n,j|V(R)|n',j'\rangle/\hbar$$

When the potential has the form of Eq.(2.7), the time-consuming matrix diagonalization needs to be performed only once. For a more general potential Eq.(4.2) will require matrix manipulations whose difficulty varies like n^3. Computational expense can therefore be a serious problem for large n, but the FPE does not suffer from this difficulty.

B. Numerical Methods for the FPE

Solution of the FPE with a classical path assumption should be very similar to the procedure outlined above for the ME. Internal state probabilities are propagated, however, by a finite difference form of the FPE rather than by Eq.(4.2). The FPE may be viewed as an approximation to the ME in the limit that the discrete quantum states are closely spaced enough to resemble a continuum. The possibly oscillatory transition rate matrix $\underset{\sim}{A}$ is also approximated by a smooth, continuous distribution, which is determined by the first and second moments of $\underset{\sim}{A}$ about the diagonal. Consequently, a numerical solution of the FPE does not require the consideration of every state, and the computational difficulty depends more on the number of degrees of freedom than the number of states. This can be a great advantage for complex collision systems where the number of open channels is very large.

The FPE is to be solved on a region with a stepped boundary since conservation of the total energy links the maximum allowed vibrational and rotational levels. This area must then be filled with a mesh or grid of discrete points at which the partial derivatives of the FPE are replaced by finite differences. It is also desirable to express the boundary conditions in a numerical fashion that is independent of the particular functional form of the coefficients. Since the FPE is derived from the ME, formulation of appropriate difference expressions and boundary conditions may be guided by a comparison with the ME. It is, therefore, suggestive that the mesh be no more closely spaced than the discrete quantum states. A typical (but simplified) situation is shown in Figure 1 where each grid point is assumed to lie on one of the quantum states. This figure is analyzed below.

Define x and y to be the continuous variables corresponding to the vibrational energy and rotational energy, respectively. Now consider the state 11 of Figure 1 and the eight states surrounding it to be typical of a point away from the boundaries. Since the FPE was obtained by an expansion through second order of the ME, it is natural that the continuous function P(x,y) be obtained by quadratic interpolation. The expressions for the partial derivatives are, therefore, obtained from the biquadratic Lagrange interpolating polynomial[10]

$$
\begin{aligned}
,y) = {} & \frac{(x-x_1)(x-x_2)}{x_{10}x_{20}}\left[\frac{P_{00}(y-y_1)(y-y_2)}{y_{10}y_{20}} - \frac{P_{01}(y-y_0)(y-y_2)}{y_{10}y_{21}} + \frac{P_{02}(y-y_0)(y-y_1)}{y_{20}y_{21}}\right] \\
& - \frac{(x-x_0)(x-x_2)}{x_{10}x_{21}}\left[\frac{P_{10}(y-y_1)(y-y_2)}{y_{10}y_{20}} - \frac{P_{11}(y-y_0)(y-y_2)}{y_{10}y_{21}} + \frac{P_{12}(y-y_0)(y-y_1)}{y_{20}y_{21}}\right] \\
& + \frac{(x-x_0)(x-x_1)}{x_{20}x_{21}}\left[\frac{P_{20}(y-y_1)(y-y_2)}{y_{10}y_{20}} - \frac{P_{21}(y-y_0)(y-y_2)}{y_{10}y_{21}} + \frac{P_{22}(y-y_0)(y-y_1)}{y_{20}y_{21}}\right] \qquad (4.5
\end{aligned}
$$

where $P_{ij} = P(x_i,y_j)$ and $x_{ij} = x_i - x_j$.

The following expressions are thus obtained by differentiating Eq.(4.5):

$$x_{10}x_{20}x_{21}\left.\frac{\partial P}{\partial x}\right|_{\substack{x=x_1\\y=y_1}} \simeq x_{10}^2P_{21} - x_{21}^2P_{01} - x_{20}(x_{10}-x_{21})P_{11} \qquad (4.6a)$$

$$x_{10}x_{20}x_{21}\left.\frac{\partial^2 P}{\partial x^2}\right|_{\substack{x=x_1\\y=y_1}} \simeq 2\left[x_{21}P_{01} - x_{20}P_{11} + x_{10}P_{21}\right] \qquad (4.6b)$$

$$x_{10}x_{20}x_{21}y_{10}y_{20}y_{21}\left.\frac{\partial^2 P}{\partial x \partial y}\right|_{\substack{x=x_1\\y=y_1}} = x_{10}^2y_{10}^2P_{22} + x_{21}^2y_{21}^2P_{00} - x_{21}^2y_{10}^2P_{02} - x_{10}^2y_{21}^2P_{20}$$

$$+ x_{21}^2y_{20}(y_{10}-y_{21})P_{01} + y_{21}^2x_{20}(x_{10}-x_{21})P_{10}$$

$$- x_{10}^2y_{20}(y_{10}-y_{21})P_{21} - y_{10}^2x_{20}(x_{10}-x_{21})P_{12}$$

$$+ x_{20}y_{20}(x_{10}-x_{21})(y_{10}-y_{21})P_{11} \qquad (4.7)$$

Approximations for $\frac{\partial P}{\partial y}$ and $\frac{\partial^2 P}{\partial y^2}$ are obtained by switching x and y in Eqs.(4.6a,b). If it is assumed that the microscopic transition rates $A(n,j;n',j';t)$ are zero for more than one step off the diagonal, it can be shown that the finite difference form of the FPE is then identical to the appropriate ME in Eq.(4.8)

$$\frac{\partial}{\partial t}P(n,j,t) = A(n,j;n+1,j,t)\left[P(n+1,j,t) - P(n,j,t)\right]$$

$$+ A(n,j;n-1,j,t)\left[P(n-1,j,t) - P(n,j,t)\right]$$

$$+ A(n,j;n,j+1;t)\left[P(n,j+1,t) - P(n,j,t)\right]$$

$$+ A(n,j;n,j-1;t)\left[P(n,j-1,t) - P(n,j,t)\right] \qquad (4.8)$$

In this connection note that the D coefficient involves microscopic transition rates that are at least two steps off the diagonal (one in n and one in j).

The finite difference form of the FPE presented here therefore matches the ME at $n-1$, n, and $n+1$ (and similarly for j). When n is equal to zero, modified approximations to the partial derivatives which match the ME at n, $n+1$, and $n+2$ should be used. Appropriate revised expressions for $\frac{\partial P}{\partial x}$ and $\frac{\partial^2 P}{\partial x \partial y}$ are obtained by evaluating the derivatives of Eq.(4.5) along the left edge

$$x_{10}x_{20}x_{21}\left.\frac{\partial P}{\partial x}\right|_{\substack{x=x_0\\y}} \simeq -x_{21}(x_{10}+x_{20})\,P(x=x_0,y) - x_{10}^2\,P(x=x_2,y) + x_{20}^2\,P(x=x_1,y) \qquad (4.9a)$$

$$0x_{20}x_{21}y_{10}y_{20}y_{21}\left.\frac{\partial^2 P}{\partial x \partial y}\right|_{\substack{x=x_0\\y=y_1}} \simeq x_{20}^2\left[y_{10}^2P_{12} - y_{21}^2P_{10} - y_{20}(y_{10}-y_{21})P_{11}\right] - x_{10}^2\left[y_{10}^2P_{22} - y_{21}^2P_{20} - y_{20}(y_{10}-y_{21})P_{21}\right] - x_{21}(x_{10}+x_{20})\left[y_{10}^2P_{02} - y_{21}^2P_{00} - y_{20}(y_{10}-y_{21})P_{01}\right] \qquad (4.9b)$$

e case $j=0$ is treated by analog, ..d at the corner point 0 0

$$0x_{20}x_{21}y_{10}y_{20}y_{21}\left.\frac{\partial^2 P}{\partial x \partial y}\right|_{\substack{x=x_0\\y=y_0}} \simeq x_{20}^2\left[y_{20}^2P_{11} - y_{10}^2P_{12} - y_{21}(y_{10}+y_{20})P_{10}\right] - x_{10}^2\left[y_{20}^2P_{21} - y_{10}^2P_{22} - y_{21}(y_{10}+y_{20})P_{20}\right] - x_{21}(x_{10}+x_{20})\left[y_{20}^2P_{01} - y_{10}^2P_{02} - y_{21}(y_{10}+y_{20})P_{00}\right] \qquad (4.10)$$

Suitable boundary conditions also need to be formulated for the upper (stepped) edge. These must satisfy the requirements that all the probabilities sum to unity while the flux $\left(\frac{\partial P}{\partial x} \text{ or } \frac{\partial P}{\partial y} \right)$ vanishes everywhere along the upper border. This last condition can be fulfilled by assigning fictitious probabilities to the layer of states immediately outside the region of interest. It should be pointed out, however, that these non-zero closed channel probabilities are only a mathematical construct with no physical meaning. Referring to Figure 1, we thus set $P_{09} = P_{08}$, $P_{19} = P_{18}$, $P_{29} = P_{18}$, $P_{28} = P_{18}$, etc. The above boundary conditions will still not insure conservation of probability; this can be accomplished by renormalizing the individual probabilities at each step in time. It is easy to see that the procedure outlined here is consistent with a statistical solution, i.e.,

$$P(n,j,t) = 1/(\text{number of open states})$$

Leakage (dissociation) can also be allowed if the fluxes through part of the upper boundary are different from zero (see paper I).

Reference to Figure 1 also reveals that the zero flux condition requires $P_{12} = P_{81}$ and $P_{35} = P_{44} = P_{53} = P_{62}$. It should be recalled that only open states are included in these calculations, and probabilities along the upper boundary may, therefore, be unreliable. This is a common situation with any finite basis set calculation. In the present case no difficulty should be encountered since the stochastic theory is developed for large systems where the upper border is likely to be far from the region of interest. In other words, most problems will be concerned with behavior in the lower left side of Figure 1 and the presence of the upper boundary will frequently not be sensed.

In view of the above, it is easily seen that propagating in time the probability of being in any specific quantum state by means of the FPE requires only the surrounding block of nine states. Thus the numerical effort of computing each "trajectory" for this two-dimensional problem goes like $9n$. More generally the dependence would be $n \times 3^N$ (n is the number of states and N is the number of degrees of freedom). Numerical computation of the FPE, like classical mechanical methods, depends more on the number of degrees of freedom than the number of quantum states. This should be a tremendous advantage when n is very large, as it is for many problems of interest. In the limit of many states, the FPE may also be treated as an exact partial differential equation rather than as a smoothed approximation to the ME. The FPE can thus be solved with a coarser mesh, resulting in additional savings in computational labor.

Considerations bearing on the choice of the time steps τ were discussed in Section II.A; for the FPE the numerical stability of the difference equations should also be taken into account. We wish to apply the von Neumann stability criterion[11] to the FPE. Assume $P\left(x_n, y_m, t\right)$ has the form

$$P\left(x_n, y_m, t\right) = \exp(in\theta)\ \exp(im\varphi)\ \exp(i\lambda t)$$

where θ, φ, and λ are some numbers. The difference equations are then presumed stable if $\exp(i\lambda t)$ is a decreasing exponential for all real θ and φ. Applying this to the atom-vibrotor FPE yields the following inequality:[12]

$$x_{10}x_{21}y_{10}y_{21} \geq \left\{ \left[x_{20}(x_{21} - x_{10})\tau B_1 - 2x_{20}\tau B_2 \right] y_{10}y_{21} \right.$$

$$\left. + \left[y_{20}(y_{21} - y_{10})\tau C_1 - 2y_{20}\tau C_2 \right] x_{10}x_{21} + 2(x_{21} - x_{10})(y_{21} - y_{10})\tau D \right\} \qquad (4.11)$$

where the indices 0, 1, 2 stand for n-1, n, n + 1, and similar indexing applies to j. The maximum value of τ allowed by Eq.(4.11) is thus a simple function of the FPE coefficients.

If the interaction is weak, Eq.(4.11) can be readily compared with the previous prescription. Expanding the exponential time propagator and assuming a tridiagonal potential matrix gives

$$\tau A(n,j;n',j';t) \simeq \begin{cases} \tau^2 |V_{nj,n'j'}|^2/\hbar^2 & |n-n'| \le 1 \text{ and } |j-j'| \le 1 \\ 0 & \text{otherwise} \end{cases}$$

Inserting this into Eq.(4.11) yields

$$\tau \le \hbar \left[|V_{nj,n+1\,j}|^2 + |V_{nj,n-1\,j}|^2 + |V_{nj,n\,j+1}|^2 + |V_{nj,n\,j-1}|^2 \right]^{-1/2}$$

which is similar to the physical criterion presented in Eq.(2.5).

V. CONCLUSION

In this paper we have formulated additional practical procedures for dealing with the stochastic equations presented in I. Molecular collisions frequently involve relatively massive particles so that the translational degree of freedom may be reasonably treated as following a classical trajectory. We have presented a formalism in which the translational degree of freedom is described by classical mechanics while the internal states are propagated by a quantum stochastic equation of motion. Considering the simplicity of the stochastic equations for the internal modes, this would seem to be an attractive conceptual model for molecular collisions. Indeed, useful qualitative information can be gained from a knowledge of the FPE coefficients, even without solving the equation, since these coefficients control the effective collisional coupling.

There are numerous techniques for calculating collisional information, and each has its own realm of applicability. Previous methods have generally proved inadequate for dealing with the scattering of relatively complex particles. For many systems of interest, the number of open channels n is too large for a fully quantal close coupling or effective Hamiltonian calculation to be practical. The expense of performing completely classical trajectory studies depends more on the number of internal degrees of freedom N than the number of states. They have the serious disadvantage, however, that all quantum effects are lost. Classical S-matrix methods[13] combine quantum interference effects with the ease of computing classical trajectories. Even with the use of effective Hamiltonians,[9] there may still be too many degrees of freedom for a classical S-matrix calculation to be feasible for many collision problems. It is hoped that the FPE, as formulated in this work,

will permit reasonable and practical scattering calculations for very complex collision systems.

Finally, the FPE is a type of partial differential equation which has been extensively studied. It was shown in I how a knowledge of the FPE coefficients and the associated boundary conditions could lead to reasonable qualitative predictions about the behavior of an inelastic collision. This paper presents a practical method for proceeding directly from the interaction potential to the coefficients of the FPE. These could then be used for qualitative interpretation or as input into numerical calculations. It is therefore hoped that a reasonably direct connection can be made between the Hamiltonian of a system and the outcome of an inelastic collision.

APPENDIX: CALCULATIONS FOR THE COLLINEAR VIBRATIONAL EXCITATION OF A MODEL He-H_2 SYSTEM

The collinear collision of an atom with a diatomic harmonic oscillator has been used frequently as a test case for various approximate methods. Calculations including certain simplifying assumptions were presented in I. When these additional approximations are removed, the solutions of the ME can be directly compared to "exact" quantum results,[14] and this is done below.

The collision system was described in I; as before the interaction potential is taken to be an exponential repulsion between the atom and the near end of the diatom. In the reduced units of Ref. 14a (except that the unit of energy is $\hbar\omega$ not $\hbar\omega/2$), the Hamiltonian is

$$E = H/\hbar\omega = P_R^2/2m + H_0/\hbar\omega + V_0 \exp(-\alpha R) \exp(\alpha x) \qquad (A.1)$$

where H_0 is the vibrational energy of the oscillator, x is the reduced displacement of the oscillator from equilibrium, R is the reduced translational coordinate, and P_R is its conjugate momentum. Since the Hamiltonian is invariant to the transformation[14b]

$$R \rightarrow R + \delta$$

V_0 may be arbitrarily set equal to E.

The finite difference form of the ME is

$$P_n(t+\tau) = \sum_m A'(n,m,t)\, P_m(t) \qquad (A.2)$$

where τ is in units of ω^{-1} and $A'(n,m,t) = \tau A(n,m,t) + \delta_{nm}$ with

$$A(n,m,t) = \left|\langle n| \exp[i\tau E \exp(-\alpha R) \exp(\alpha x)] |m\rangle\right|^2 \qquad (A.3)$$

The matrix elements of $\exp(\alpha x)$ are

$$\langle n|\exp(\alpha x)|m\rangle = \left(\frac{n!}{m!}\right)^{1/2} (\alpha 2^{-1/2})^{m-n} \exp(\alpha^2/4) L_n^{m-n}(-\alpha^2/2) \qquad (A.4)$$

for $m \geq n$ ($L_n^m(x)$ is the associated Laguerre polynomial). Given values of τ and E, the rates in Eq.(A.3) are then conveniently obtained by numerically exponentiating the matrix whose n,m-th element is

$$i\tau E \exp(-\alpha R) \langle n| \exp(\alpha x) |m\rangle$$

The ME was solved by the procedure outlined in Section IV.A. A fifth order, variable step size Adams-Moulton predictor-corrector algorithm[15] was used to compute the classical trajectory for the R degree of freedom. At each step energy was forced to be conserved by setting

$$\dot{R}(t) = \text{sign}\,(P_R) \times \left\{2\left[E - \langle H_0/\hbar\omega\rangle - E \exp(-\alpha R) \langle \exp(\alpha x)\rangle\right]/m\right\}^{1/2} \qquad (A.5)$$

while P_R was predicted by integrating

$$\dot{P}_R = +\alpha E \exp(-\alpha R) \langle \exp(\alpha x)\rangle \qquad (A.6)$$

from t to $t+\tau$ (cf. Eqs.(4.3),(4.4)). The expectation values in these equations are given by

$$\langle H_0/\hbar\omega \rangle = \sum_n (n+1/2)\, P_n(t)$$

$$\langle \exp(\alpha x) \rangle = \sum_{n,m} \sqrt{P_n(t)\, P_m(t)}\ \langle n|\exp(\alpha x)|m\rangle$$

Since P_R is only needed for determining the sign of $\dot{R}$, it does not matter that repeated application of Eq.(A.6) will not conserve the total energy. At the beginning and end of each step, P_R/m was set equal to $\dot{R}$ computed from Eq.(A.5).

Each trajectory is started in some initial state n_0 with R set equal to some large value outside the range of the potential. The time steps τ should be given by (cf. Eq.(2.5))

$$\tau(t) = \sum_n P_n(t) \left\{ E \exp\left[-\alpha R(t)\right] \left[\sum_m (n-m)^2 \left| \langle n \exp(\alpha x) | m \rangle \right|^2 \right]^{1/2} \right\}^{-1} \qquad (A.7)$$

when in the strong interaction region. This equation is not applicable for large R where the interaction is weak and it predicts steps much too large. As a practical matter then the time step at the start of the trajectory was given some value τ_0, just larger than the estimated minimum time from Eq.(A.7). This was done to insure that the strong interaction region was not bypassed in the integration. When Eq.(A.7) predicted a smaller value than τ_0, this smaller value was used.

Calculations were performed[16] for the parameter set $m = 2/3$, $\alpha = 0.314$ at $E = 8.0$; and for $m = 2/3$, $\alpha = 0.30$ at $E = 10.0$. The two values of α were necessary because of differences in the calculations of Refs. (14a) and (14b). Results are plotted in Figures 2 and 3 along with the corresponding quantum values. It may be seen that the stochastic curves seem to represent the quantum mechanical transition probabilities with the oscillations averaged out. This result is not surprising in view of the removal of phase interferences in the stochastic theory. It should also be pointed out that the collinear harmonic oscillator model apparently exhibits an anomalously large amount of oscillation. Indeed quantum calculations for a Morse oscillator show much less of this kind of structure.[14b].

Calculations were also carried out at energies below $E = 8$. However, these results were in generally poor agreement with the quantum values for E less than 6.0. This is not unexpected since the stochastic theory should be best where there are a large number of strongly coupled states.

The procedure used here for conserving energy no longer guarantees the satisfaction of microscopic reversibility $\left(\underline{i.e.},\ P_{n_1 \to n_2}(E) = P_{n_2 \to n_1}(E)\right)$. However for classically allowed transitions, the probabilities for excitation and deexcitation were still in reasonable agreement. In contrast, the probability of deexcitation is much smaller (and more realistic than the excitation probabilities) when the transitions were classically forbidden. The origin of this phenomenon is unclear.

ACKNOWLEDGMENTS

Acknowledgment is made to the Office of Naval Research and the Petroleum Research Fund administered by the American Chemical Society for partial support of this research. We also gratefully acknowledge Professor G. Bienkowski for several helpful discussions.

REFERENCES

* Alfred P. Sloan Fellow, Camille and Henry Dreyfus Teacher-Scholar.

1. S. Augustin and H. Rabitz, J. Chem. Phys. 64, 1223 (1976).
2. See, for example, H. Rabitz, "Effective Hamiltonians in Molecular Collisions," Modern Theoretical Chemistry III, W. H. Miller, Ed. (Plenum, 1976) in press.
3. This is similar in spirit to the approach of K. McCann and R. Flannery, Chem. Phys. Lett. 35, 124 (1975).
4. θ and φ are the polar and azimuthal angles, respectively, of $\vec{r}$ measured from space-fixed axes.
5. Operators of this type are discussed by L. Infeld and T. E. Hull, Rev. Mod. Phys. 23, 21 (1951).
6. The body-fixed reference frame is a rotating set of coordinates whose z axis is constrained to be coincident with the vector $\vec{R}$.
7. (a) R. Pack, J. Chem. Phys. 60, 633 (1974).
   (b) P. McGuire and D. Kouri, J. Chem. Phys. 60, 2488 (1974).
   (c) R. B. Walker and J. C. Light, Chem Phys. 7, 84 (1974).
8. H. Rabitz, J. Chem. Phys. 57, 1718 (1972).
9. S. Augustin and H. Rabitz, J. Chem. Phys. 65, 0000 (1976).
10. See, for example, E. Isaacson and H. B. Keller, Analysis of Numerical Methods, (Wiley, New York, 1966) p. 295. Extensions to higher dimensions are obvious.
11. P. R. Garabedian, Partial Differential Equations, (Wiley, New York, 1964) p. 476.
12. If the D term is ignored, this is the same as the condition that the difference equations be of positive type. See, for example, G. E. Forsythe and W. R. Wasow, Finite Difference Methods for Partial Differential Equations, (Wiley, New York, 1960) p. 108.

13. W. H. Miller, Adv. Chem. Phys. 25, 69 (1974) and references contained therein.

14. (a) D. Secrest and B. R. Johnson, J. Chem. Phys. 45, 4556 (1966).

(b) A. P. Clark and A. S. Dickinson, J. Phys. B 6, 164 (1973).

15. W. H. Miller and T. F. George, J. Chem. Phys. 56, 5668 (1972). In this application, however, step sizes were not predicted by the estimate of the truncation error.

16. The complete matrix of transition probabilities at E = 10.0 required 14.4 seconds of computer time on an IBM 360/91.

Figure Captions

Figure 1.

A set of mesh points for the solution of an atom-vibrator FPE. The equation is to be solved in the shaded region while the layer of closed states outside of the upper edge is used to formulate the boundary conditions. The number of states and their spacings are intended for illustrative purposes only and should not be construed to represent any real system. The continuous variables x and y correspond to the vibrational energy and rotational energy, respectively.

Figure 2.

Plot of transition probabilities from initial states n_o as a function of final state n ($P_{n_o \rightarrow n}$) for E = 8. These are for the collinear oscillator problem with $\alpha = 0.514$ and $m = 2/3$. The solid lines connect the quantum values of Clark and Dickinson[14b] while the open circles are the stochastic results of this work.

Figure 3.

The same as Figure 2 for E = 10 except that $\alpha = 0.30$. Quantum results are those of Secrest and Johnson[14a].

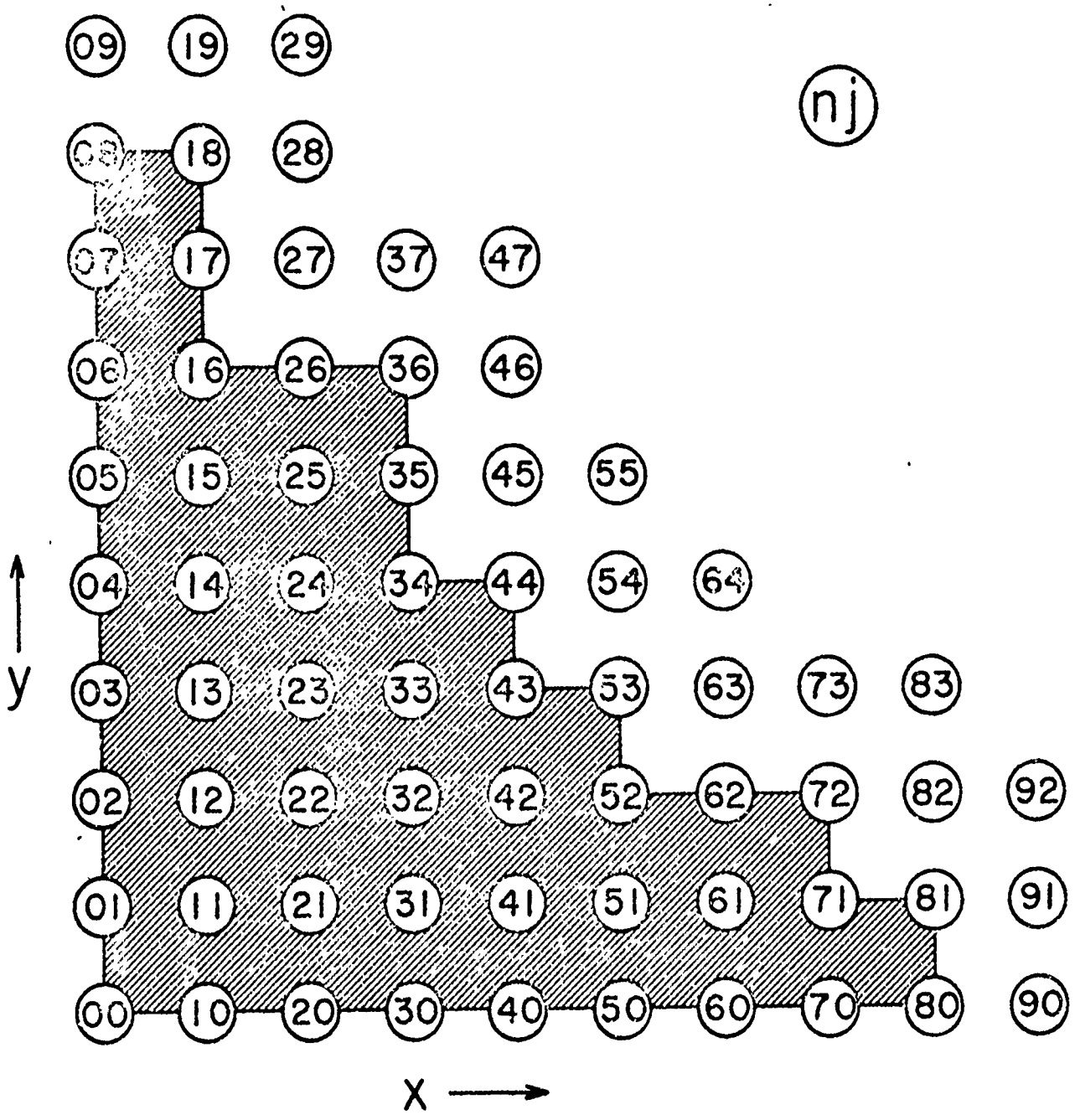
09
19
29
nj
08
18
28
07
17
27
37
47
06
16
26
36
46
05
15
25
35
45
55
04
14
24
34
44
54
64
y
03
13
23
33
43
53
63
73
83
02
12
22
32
42
52
62
72
82
92
01
11
21
31
41
51
61
71
81
91
00
10
20
30
40
50
60
70
80
90
X

Fig. 1

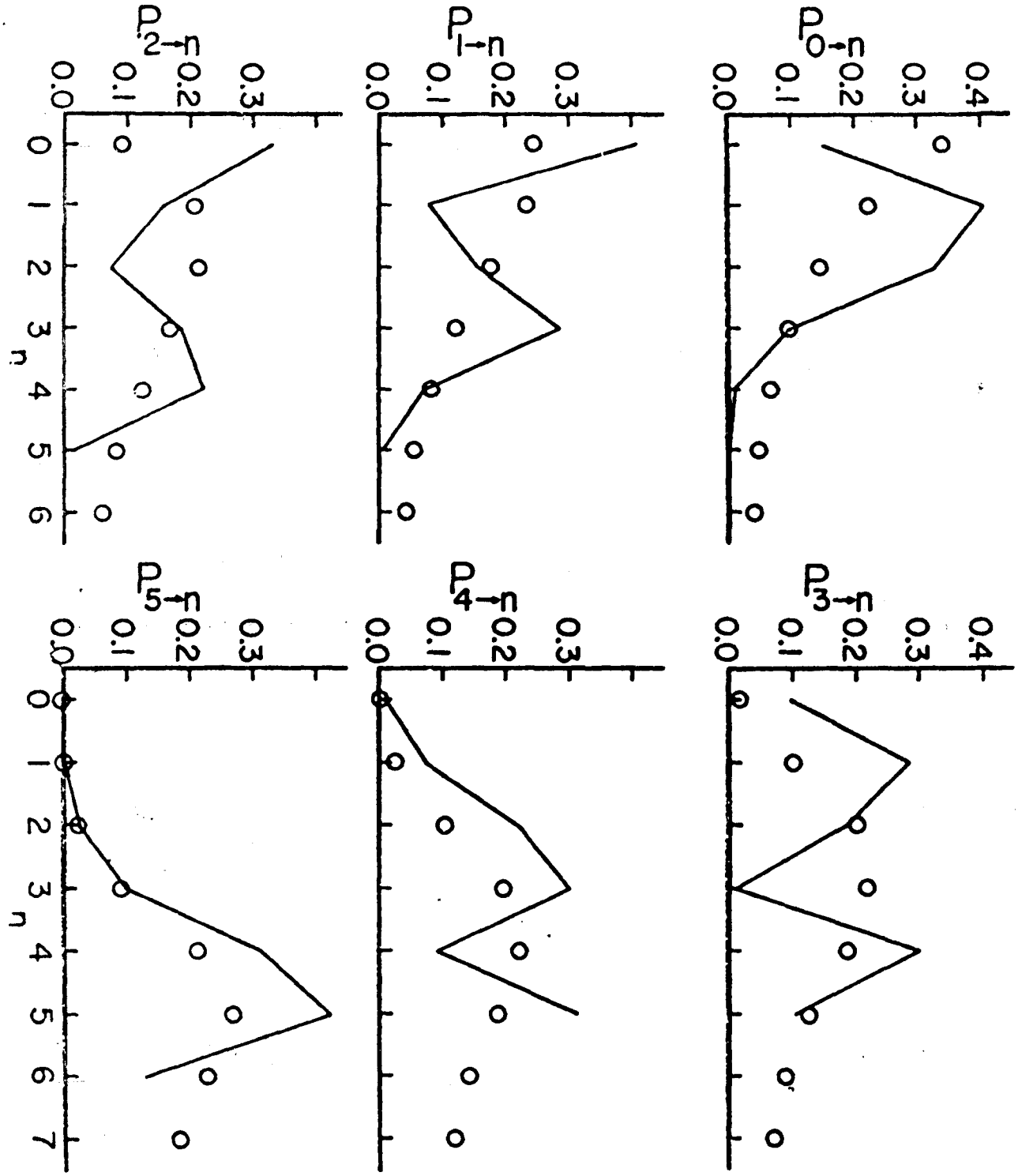
$P_0 \rightarrow f$
$P_1 \rightarrow f$
$P_2 \rightarrow f$
$P_3 \rightarrow f$
$P_4 \rightarrow f$
$P_5 \rightarrow f$
0.0
0.1
0.2
0.3
0.4
n

Fig. 2

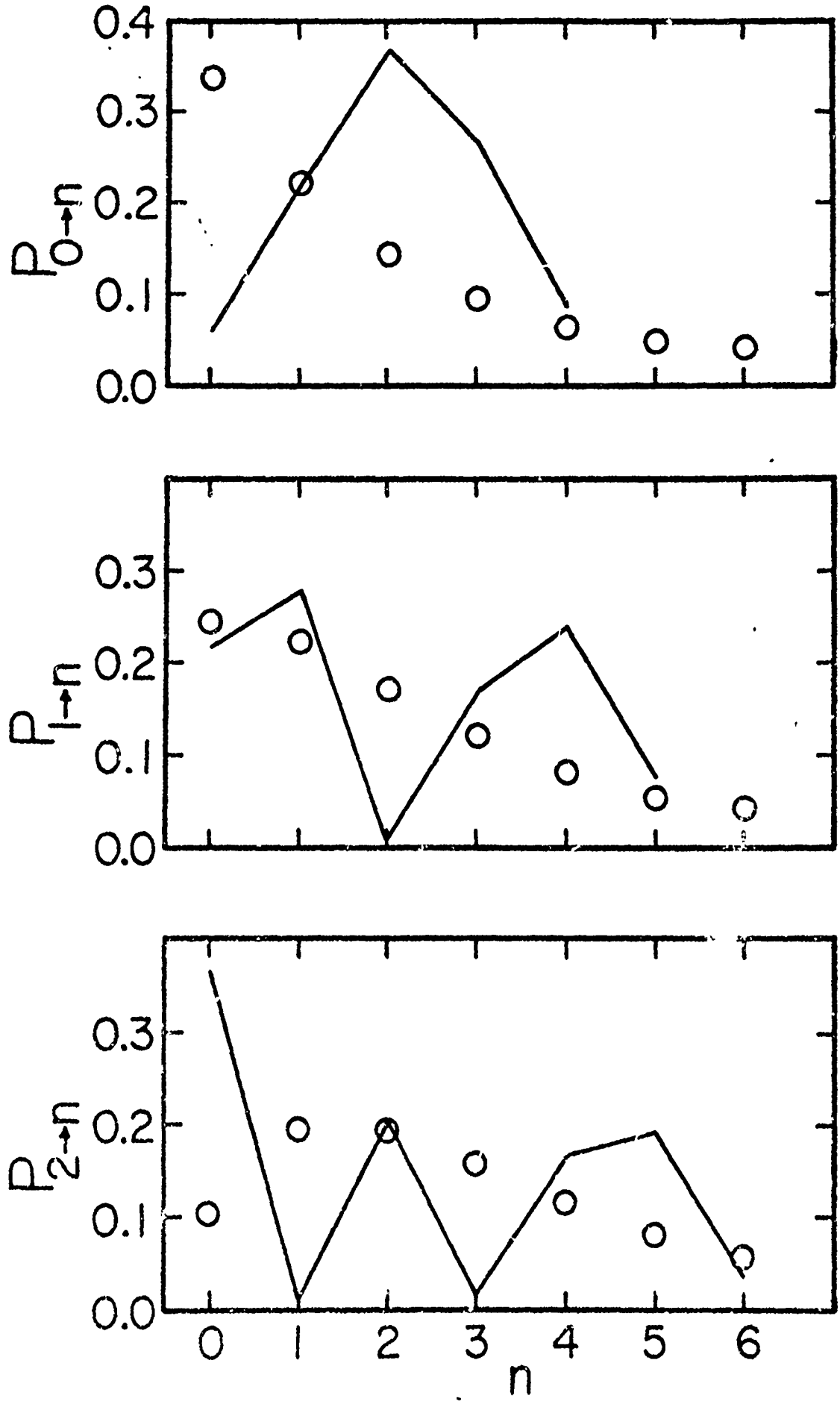

Fig. 3